Study of direct photon production in Pb-Pb collisions at $\sqrt{s_{NN}} = 5.02$ TeV with ALICE experiment's Photon Spectrometer(PHOS) at Large Hadron Collider

Sushobhan Kumar Mandal

National Center for Nuclear Research

Warsaw, Poland

23 October, 2025

Standard model and strong interaction

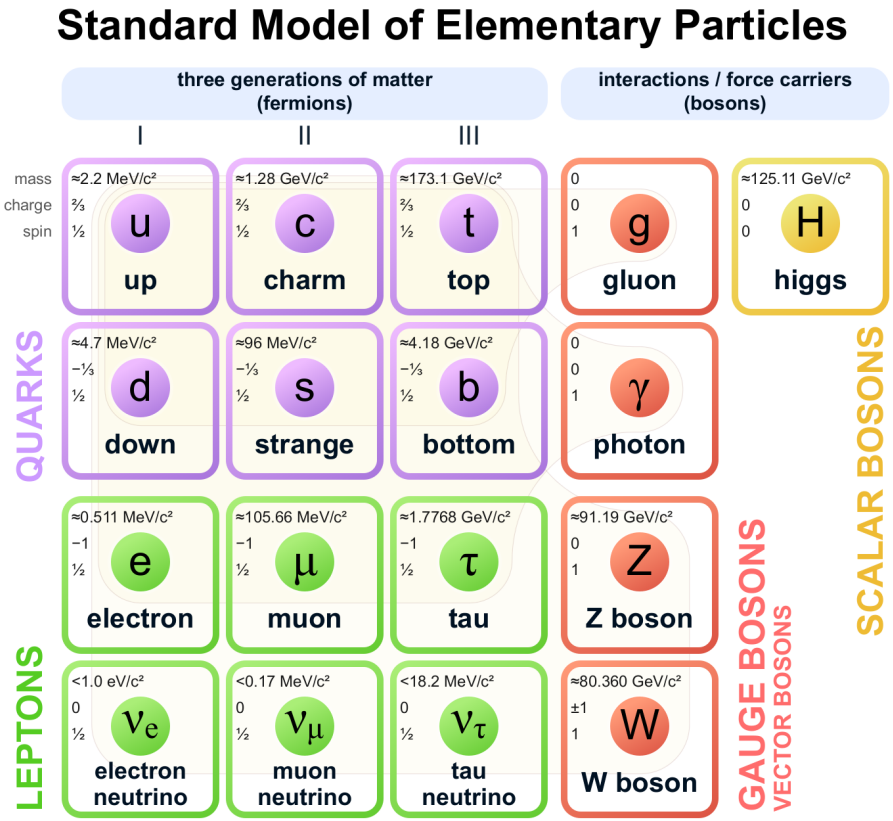

- **Quarks & gluons** carry three **color charges:** R, G, B
- **Gluons** mediate the strong interaction — linking quarks *and each other*
- **Bound states** of quarks form ordinary matter: baryons, mesons, etc.

Strength Comparison — The **strong force** [range: 10^{-15}m] is hundred ($\sim$137) times stronger than the *EM force* [range: ∞]

and million times ($\sim 10^6$) stronger than the *weak force* [range: 10^{-18}m].

Features of Quantum Chromodynamics (QCD)

- **Color confinement** — *no free color charges* in the nature
- **Chiral symmetry breaking** — ∼99% of the proton mass[938 MeV] comes from **QCD interaction** (not bare quark masses[10 MeV])
- **Asymptotic freedom:** Quarks and gluons behave like **free particles** at very **high interaction energies**. The **p**erturbative QCD works

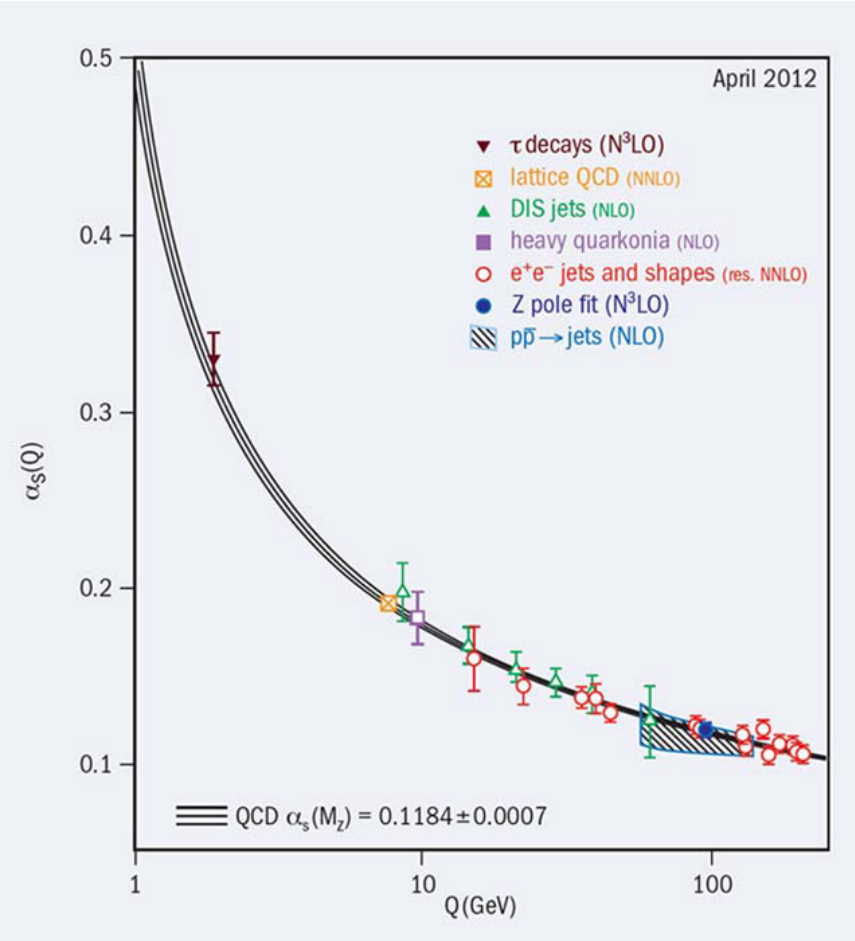

Running coupling constant $\alpha_s(Q^2) = \frac{4\pi}{\beta_0 \ln(Q^2/\Lambda^2)}$

(Gross, Wilczek, Politzer — **Nobel 2004**)

[2] Figure 3 in S. Bethke, "World Summary of α_s (2012)", MPP-2012-132, arXiv:1210.0325.

Phase transition in QCD and Quark–Gluon Plasma (QGP)

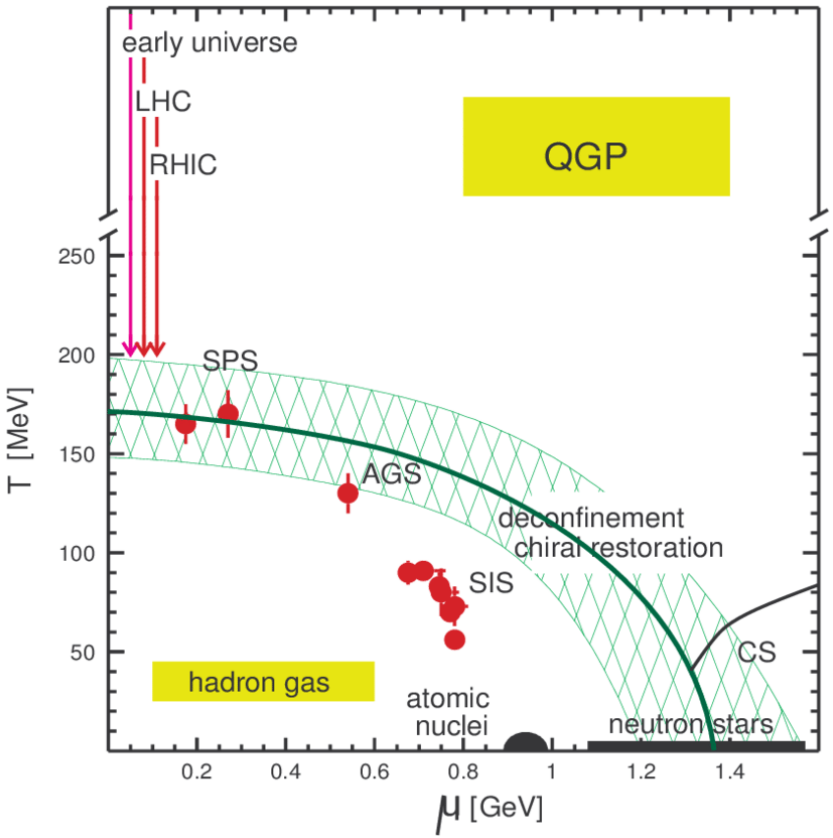

- At **high energy density (∼1 GeV/fm^3)**[1]
- or at **high temperature (∼170 MeV)**[4] (or both),

  ⇒ Hadronic matter becomes a **deconfined, fluid-like phase** of **quarks and gluons**

- At finite μ_B, lattice QCD fails (*sign problem*).
  The phase diagram must be explored by **comparing experimental results** with **effective models**.

[3] Karsch, *Lect. Notes Phys.* 209 (2002), hep-lat/0106019; Borsanyi et al., *JHEP* 1009 (2010) 073 [arXiv:1005.3508].

Evolution of collision medium and probes of QGP

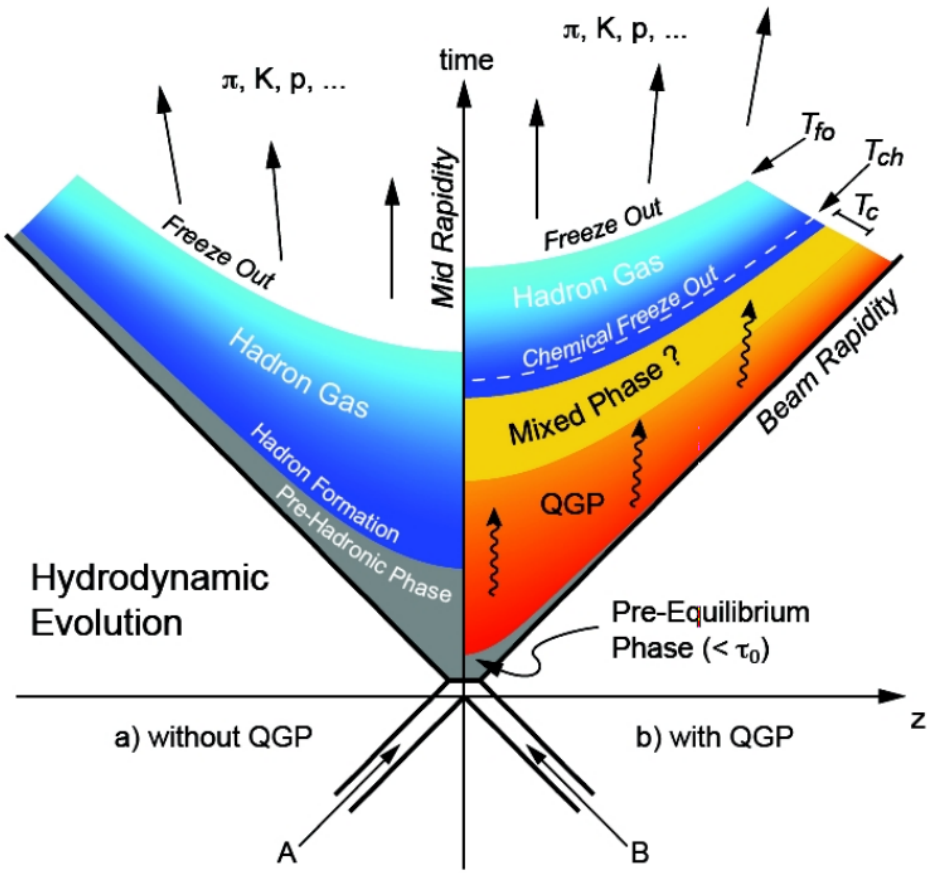

- **Jet quenching** (Energy modification of high-p_T jets)
- **Di-lepton production** ($q\bar{q} \to \mu\bar{\mu}$)
- **Direct photon production** ($q\bar{q} \to g\gamma$, $qq \to qq\gamma$ etc.)
- Others: Strangeness enhancement ($q\bar{q} \to s\bar{s}$, $g\bar{g} \to s\bar{s}$), Charmonium suppression (J/ψ suppression) etc.

[1] https://particlesandfriends.wordpress.com/2016/10/14/evolution-ofcollisions-and-qgp/

Source of photons in the different stages of evolution

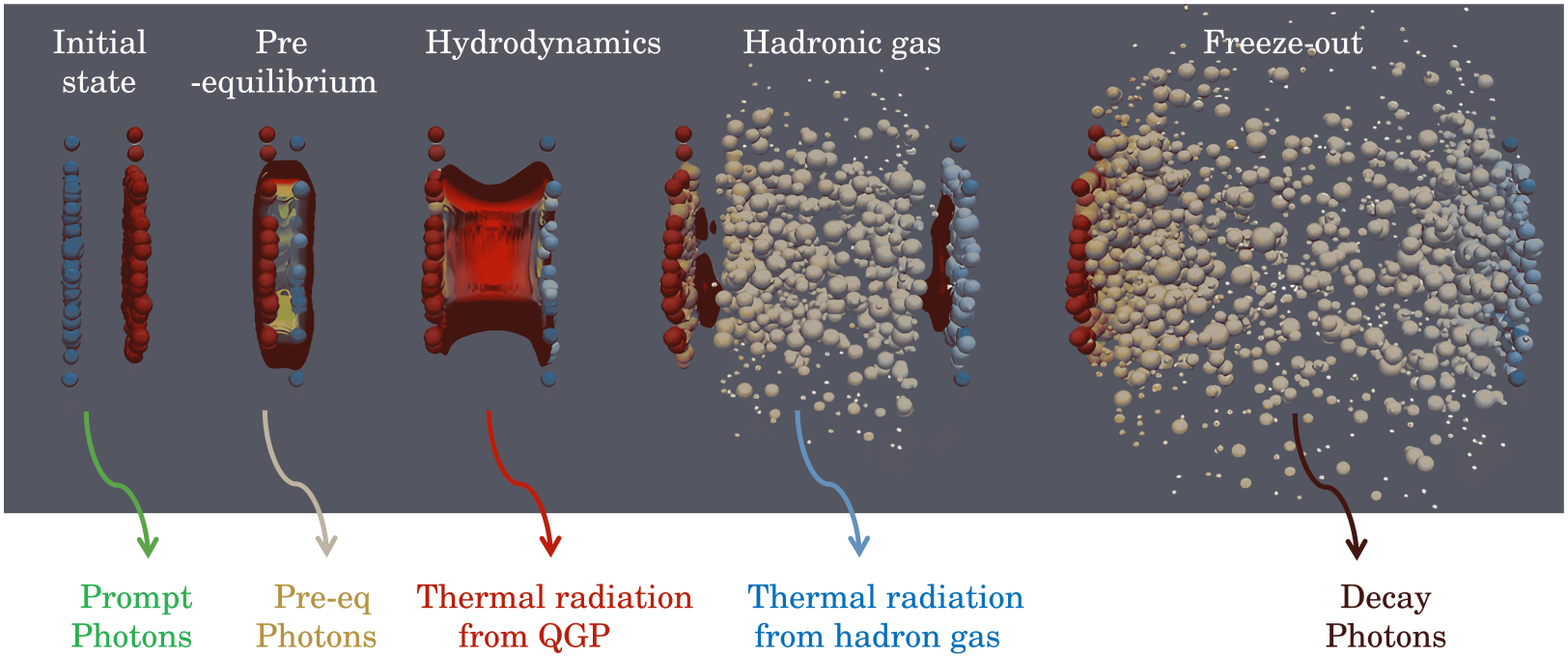

- Photons emerge **undistorted** from the strongly interacting medium, providing direct access to its temperature, flow, and density throughout the system's evolution.

[4] picture: madai colab;

Direct photon study in heavy-ion collisions

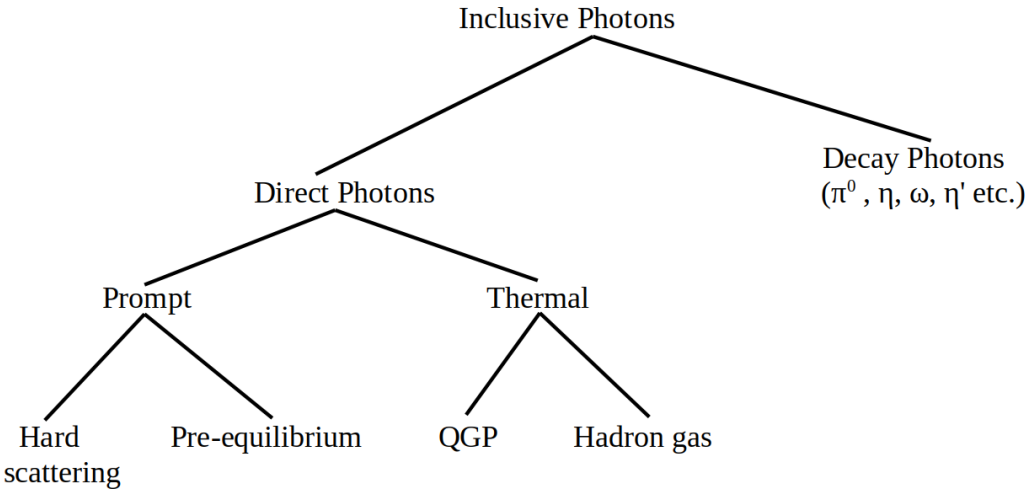

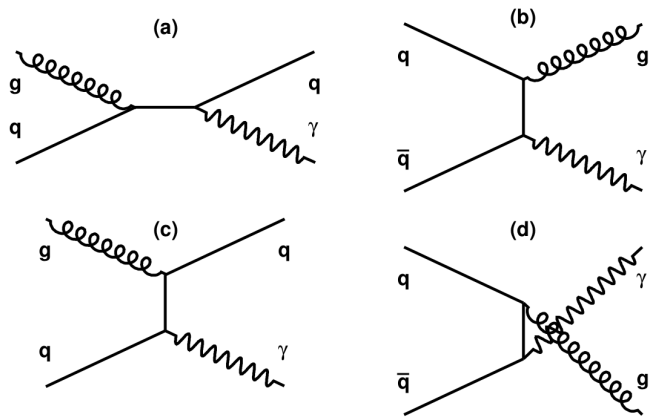

- **Hard QCD photons** : calculated via **pQCD**
- **Pre-equilibrium photons** : estimated from *non-equilibrium QCD models*
- **QGP and Hadron gas photons** : obtained from *hydrodynamic models*
- **Decay photons** : derived from *meson decay param.* and *scaling*

Figure: Prompt photon production in Compton scattering and pair annihilation processes

Large Hadron Collider and A Large Ion Collider Experiment (ALICE)

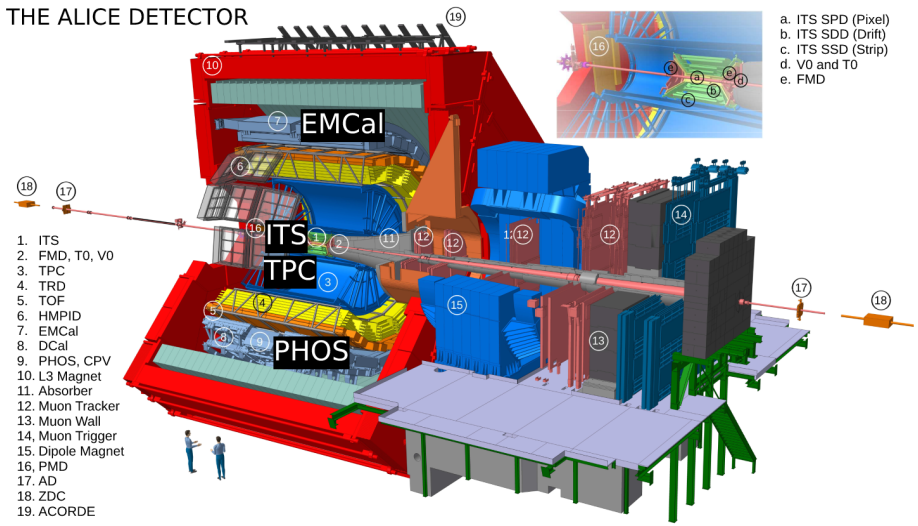

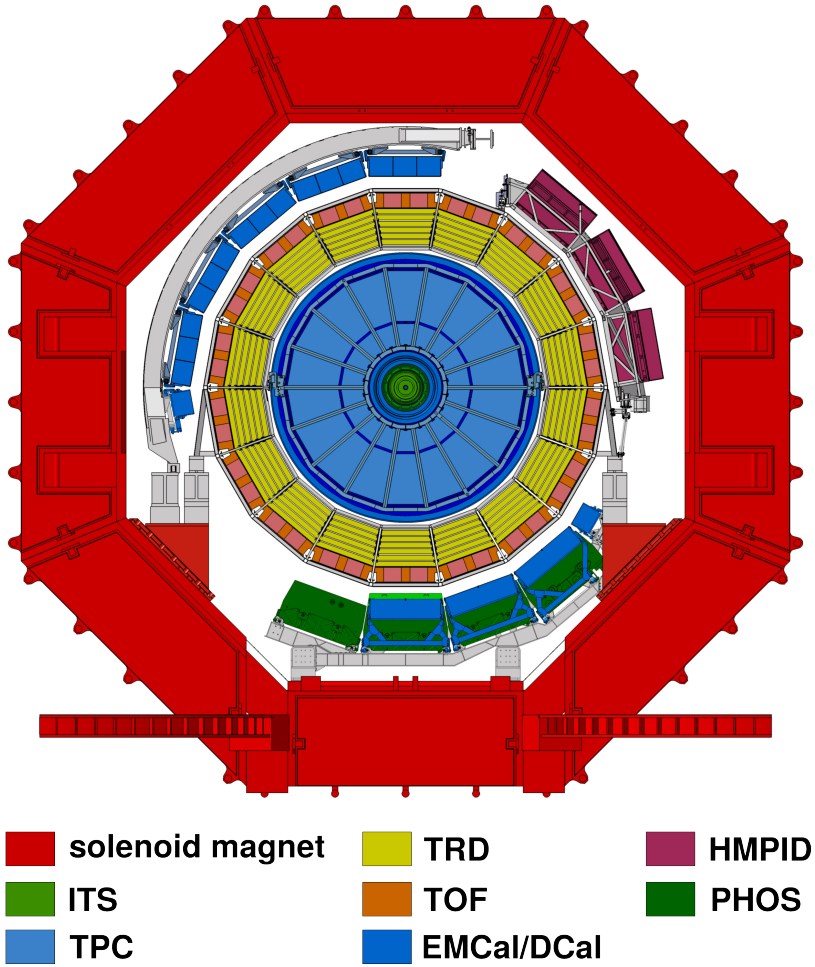

[1] cern.ch, alice-collaboration.web.cern.ch

PHOton Spectrometer(PHOS)

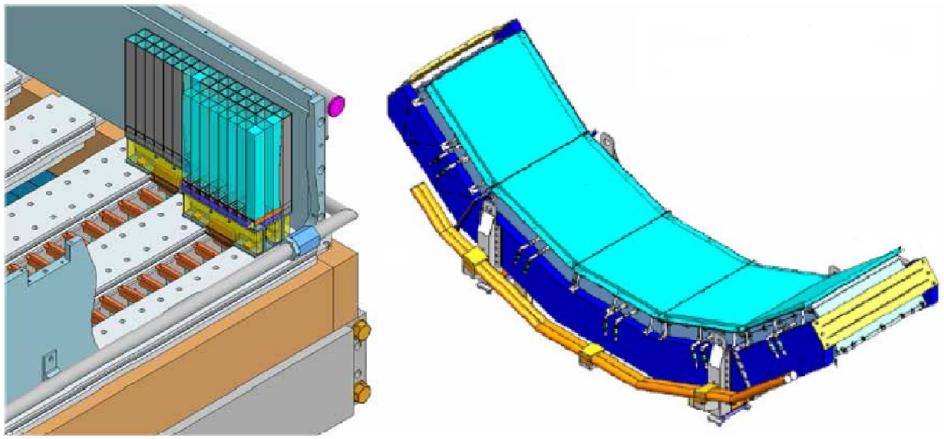

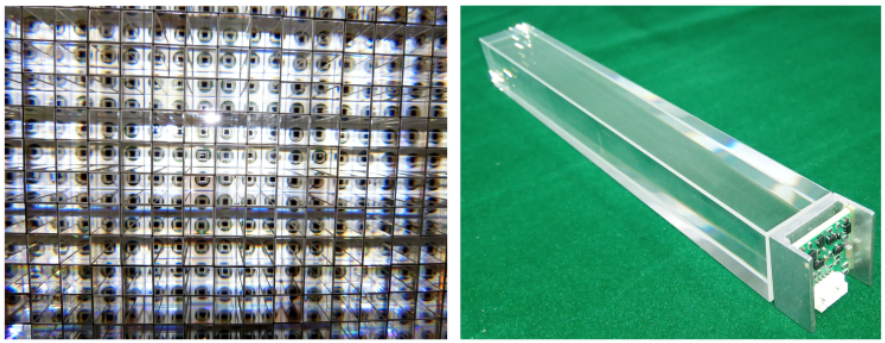

Figure: PHOS cell matrix[left]; $PbWO_4$ crystal, APD(Avalanche Photo Diode) detector and preamplifier[right]

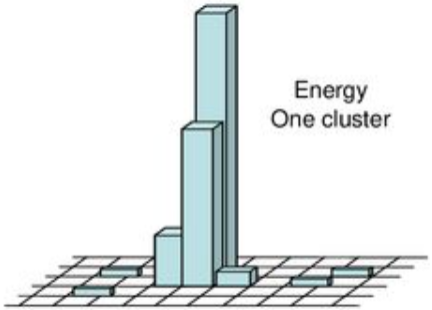

- $\sim$80% of the total cluster energy is deposited in the central cell
- Good at measuring both low energy range and high energy range : 100 MeV to 100 GeV
- At energy range $>$1GeV, the precision is approx. given by $\frac{\sigma_E}{E} = \frac{3\%}{\sqrt{E}} \pm 0.8\%$

[1] alice-collaboration.web.cern.ch

Collision centrality : $\left(\frac{spectator}{All}\right)$

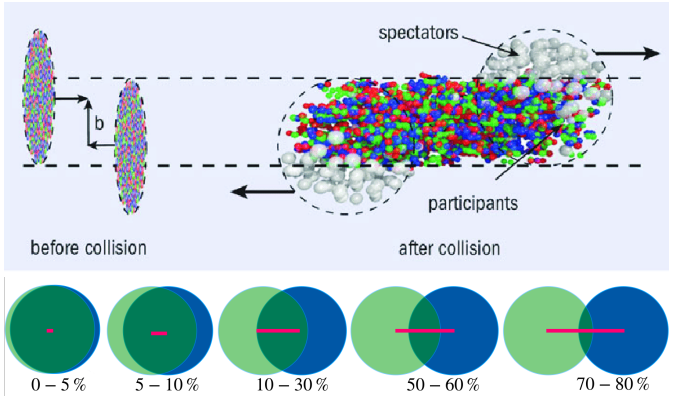

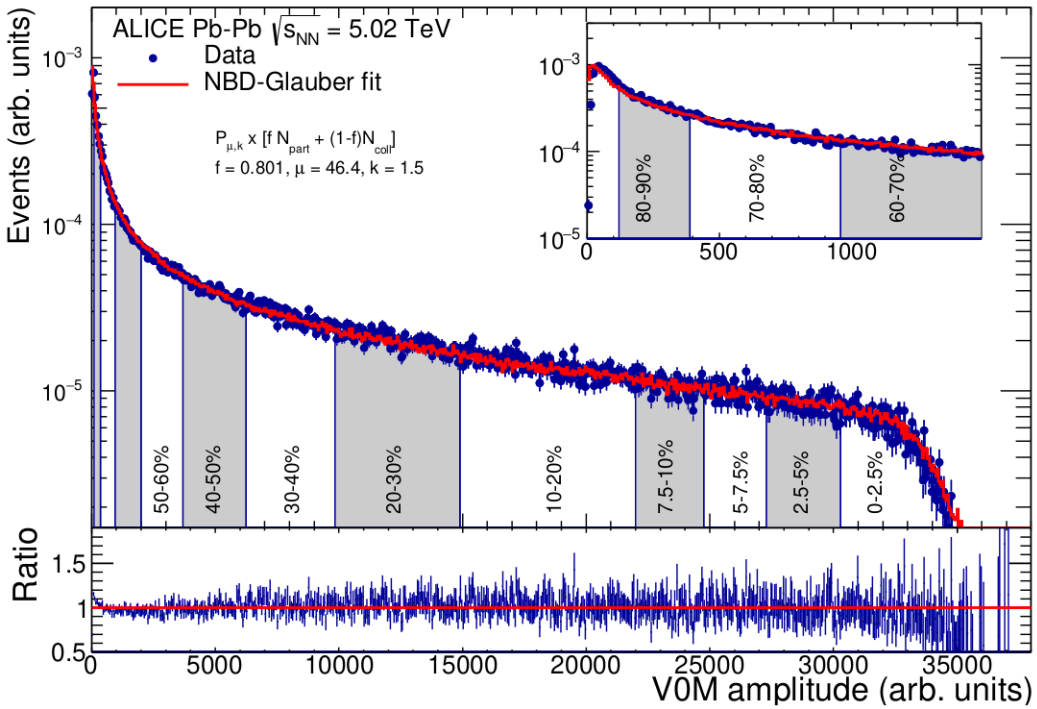

[1] Centrality determination in heavy ion collisions, ALICE-PUBLIC-2018-011

Statistics of the data, events and clusters selection

Run period	Range of run numbers	Number of selected runs	Total statistics
LHC18r	296690-297624	58	41.234×10^6
LHC18q	295581-296623	131	64.970×10^6

Event selection criterion

- To avoid pile-up of events we impose the following restrictions: **Number of vertex=1**;
- Z-coordinate of the vertex $\leq$10.0 cm.
- To exclude false signals, we choose the **number of contributors** (reconstructed charged particle tracks)$\geq$1.

Cluster selection criterion

- minimum energy of **E** $\geq$ **0.3 GeV**
- minimum number of cells **Ncells** $\geq$ **3**
- time of flight of the photons TOF $\leq$ 12.5 ns
- size of the cluster $\geq$ 0.1 cm

Raw yield of clusters in PHOS for LHC18r (different centralities)

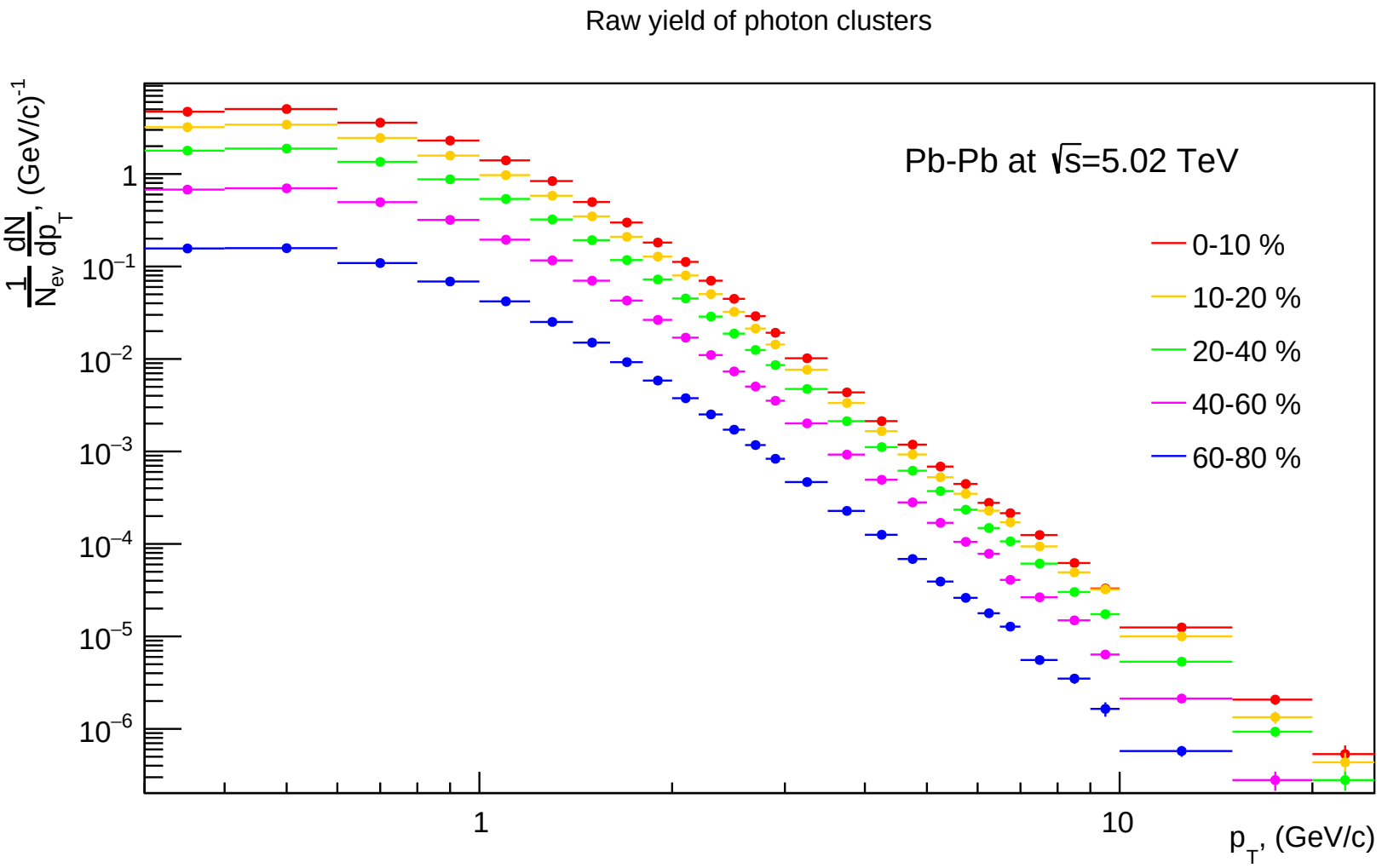

Reconstruction of the photon spectrum with PHOS:Inclusive photons(γ^{inc})

Invariant yield of photons is found as

$$E\frac{d^3N_{\gamma\,inc}}{dp^3} = P_\gamma \times \frac{1}{\epsilon_\gamma} \times \left(\frac{1}{N_{\text{ev}}} \times \frac{1}{2\pi} \times \frac{1}{p_{\text{T}}}\frac{d^2N_{PHOS}}{dp_{\text{T}}dy}\right) \tag{1}$$

P_γ - purity of the photon sample, number of PHOS photons produced by γ particles divided by the number of all PHOS photons:

$$P_\gamma = \frac{N_{\gamma\ PHOS}}{N_{PHOS}} \tag{2}$$

ϵ_γ - efficiency of the γ detection, ratio of γ clusters in PHOS to the number of γ-s produced in the collisions:

$$\epsilon_\gamma = \frac{N_{\gamma\ PHOS}}{N_{\gamma\ All}} \tag{3}$$

Contamination in the photon samples

$$N_{cluster} = N_{\gamma} + N_{e^{\pm}} + N_{\pi^{\pm}} + N_{K^{\pm}} + N_{p} + N_{\bar{p}} + N_{n} + N_{\bar{n}} + N_{K^{0}_{L}} + N_{K^{0}_{S}} + ...$$

- Using **MC data** we can simulate the clusters due to other particles
- **CPV cut:** The clusters are removed if they are too close to the charged tracks($e^{\pm}, \pi^{\pm}, K^{\pm}, p$) measured by CPV [and ITS detector]
- **Dispersion cut:** Based on cluster characteristics (e.g. shower shape) we minimize contaminations of other particles including neutral particles

The ionization loss in $PbWO_4$ for $\mu^{\pm}$ is very small compared to energy cut(< 0.3 GeV) for event selection

PHOS sample purity using vertex photons

$$Purity(p_T) = \frac{N_{\gamma_{clusters}}(p_T)}{N_{all_{clusters}}(p_T)}$$

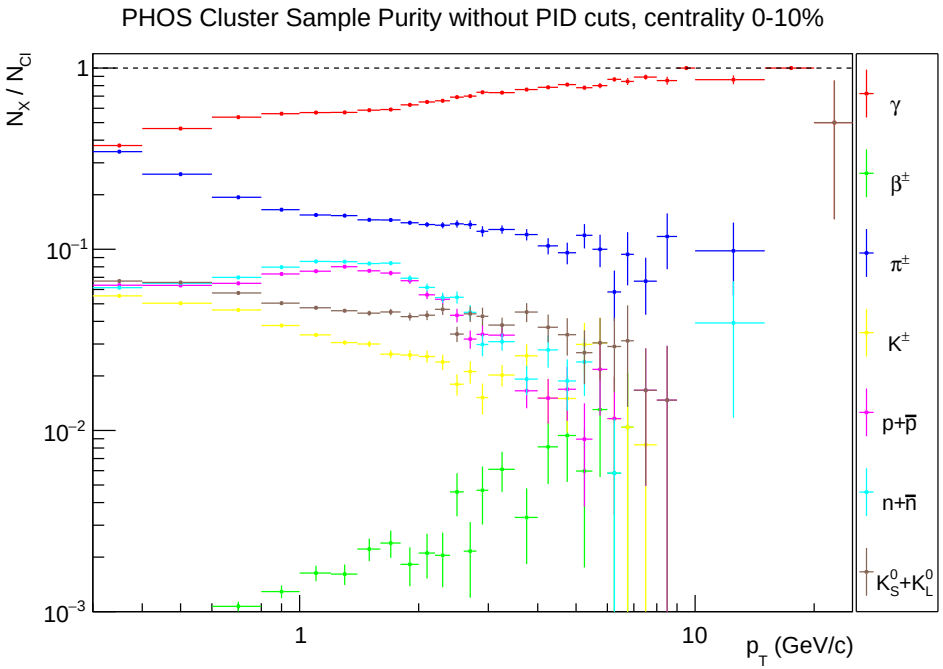

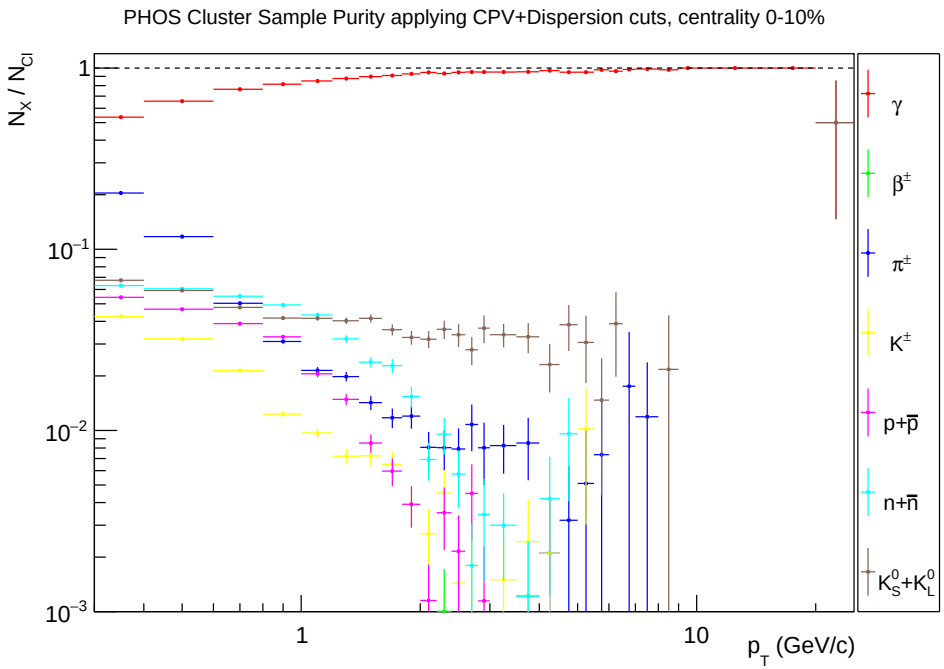

Efficiency of photon detection in PHOS

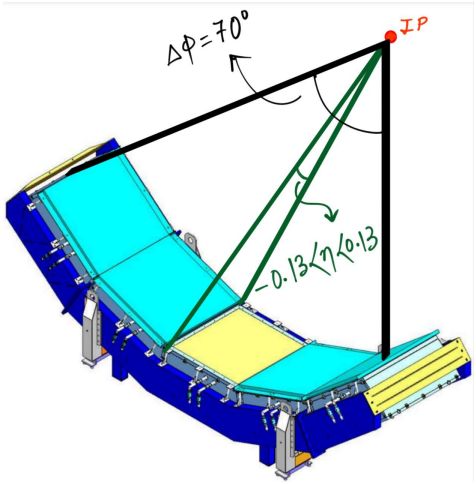

Figure: Modules of the PHOS detector and its angular coverage

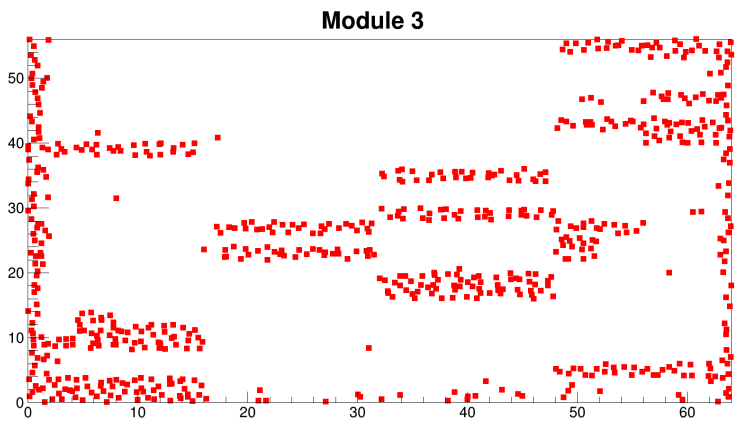

Figure: Red squares represent Bad channels, LHC18r Module3

- For photons emitted at mid-rapidity, $|y| < 0.5$, $0 < \phi < 2\pi$, only **5.1% of all photons** fly into the PHOS solid angle
- Photons can be caught inside **bad electronic** channel
- Converted into **electron-positron** pair, which is **deflected** by magnetic field
- Entirely **absorbed** or dispersed by material of **tracking detector**
- Photons may impinge on calorimeter surface **close to a charged particle**

Efficiency for different centralities (applying CPV+Dispersion cut)

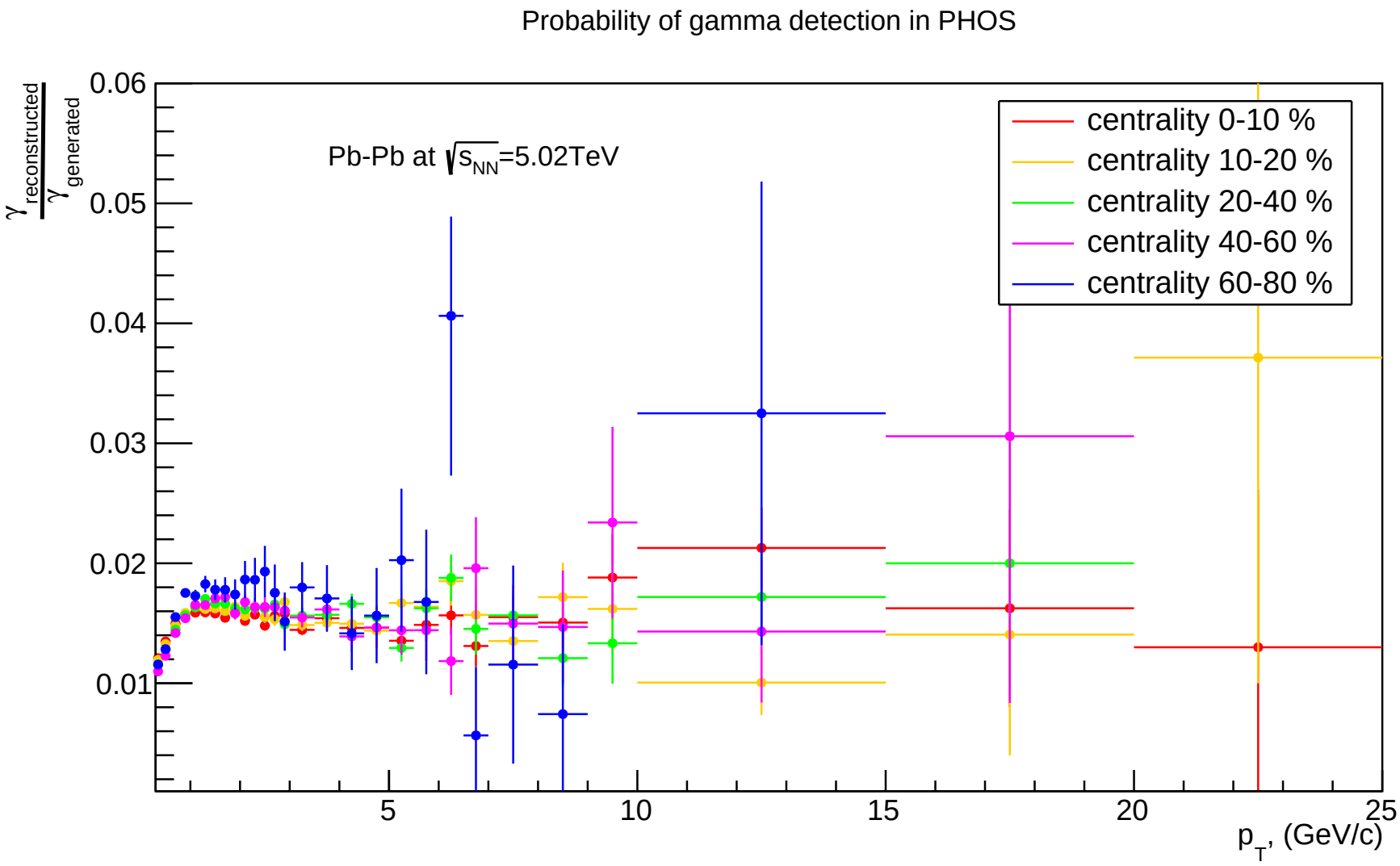

Embedding: measure photon efficiency under **real** Pb–Pb conditions

- **What it is** — Embed a *simulated* photon (or π^0) at the interaction point into a *real* recorded event at the **digit/raw** level, then re-run reconstruction.
- **Why it matters** — Captures **true occupancy, overlaps, noise, bad channels etc.** that pure MC cannot fully reproduce in heavy-ion conditions.
- **What we get** — A **data-driven** $\varepsilon_\gamma(p_T)$ (acceptance $\times$ efficiency).

Simulated photon + Real Pb–Pb digits $\Rightarrow$

Superimposed digits $\Rightarrow$ Reconstruction $\rightarrow$ clusters

Embedding efficiency

$$\varepsilon_\gamma(p_T) = \frac{N_{\text{clu}}^{\text{After Emb}}(p_T) - N_{\text{clu}}^{\text{Before Emb}}(p_T)}{N_\gamma^{\text{Generated}}(p_T)}$$

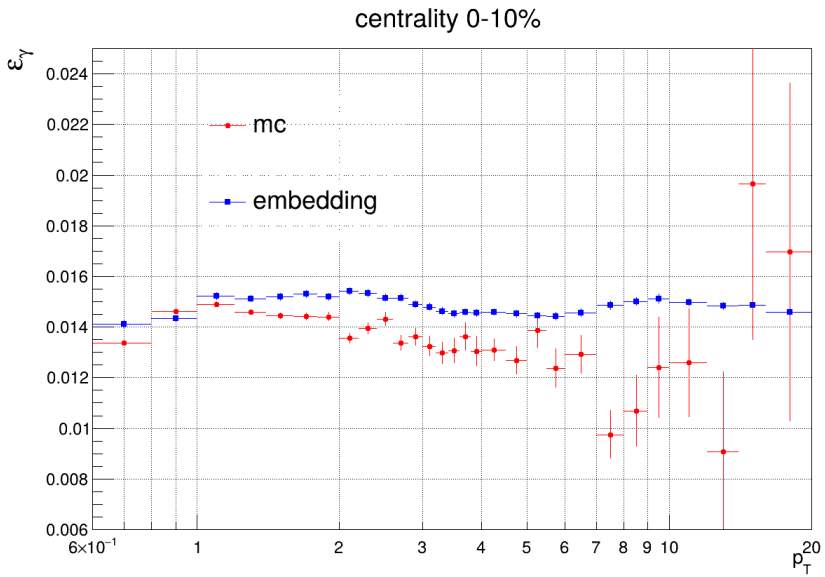

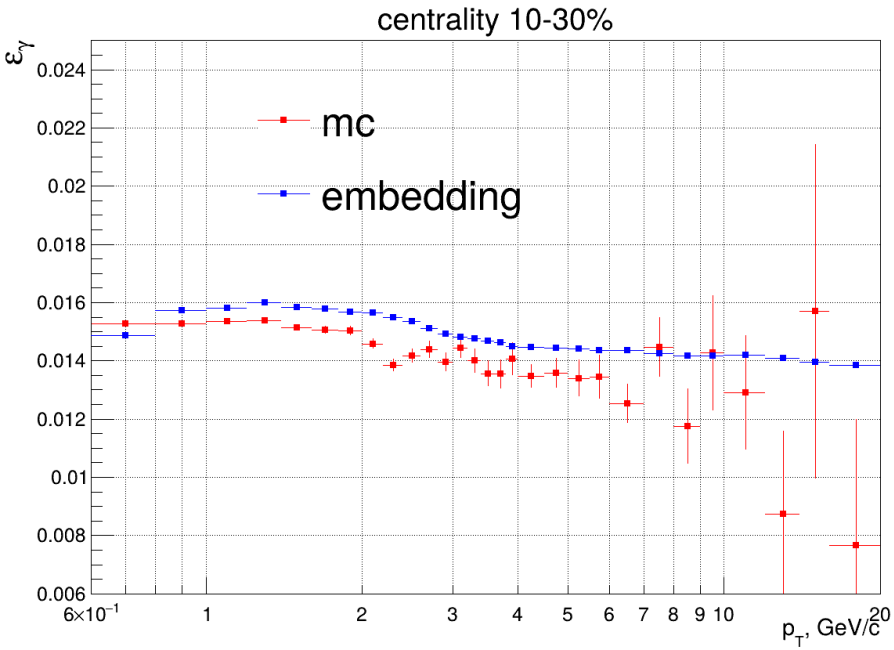

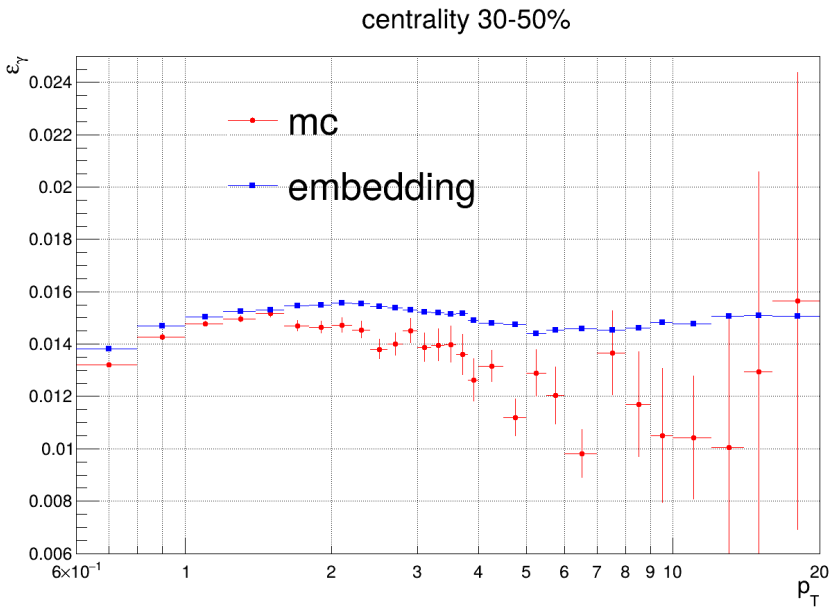

Invariant yield of inclusive photons : Different centralities

$$P_\gamma \times \frac{1}{\epsilon_\gamma} \times \left(\frac{1}{N_{\text{ev}}} \times \frac{1}{2\pi} \times \frac{1}{p_{\text{T}}} \frac{d^2 N_{PHOS}}{dp_{\text{T}} dy} \right) \tag{4}$$

Inclusive Photon Spectra for different centralities

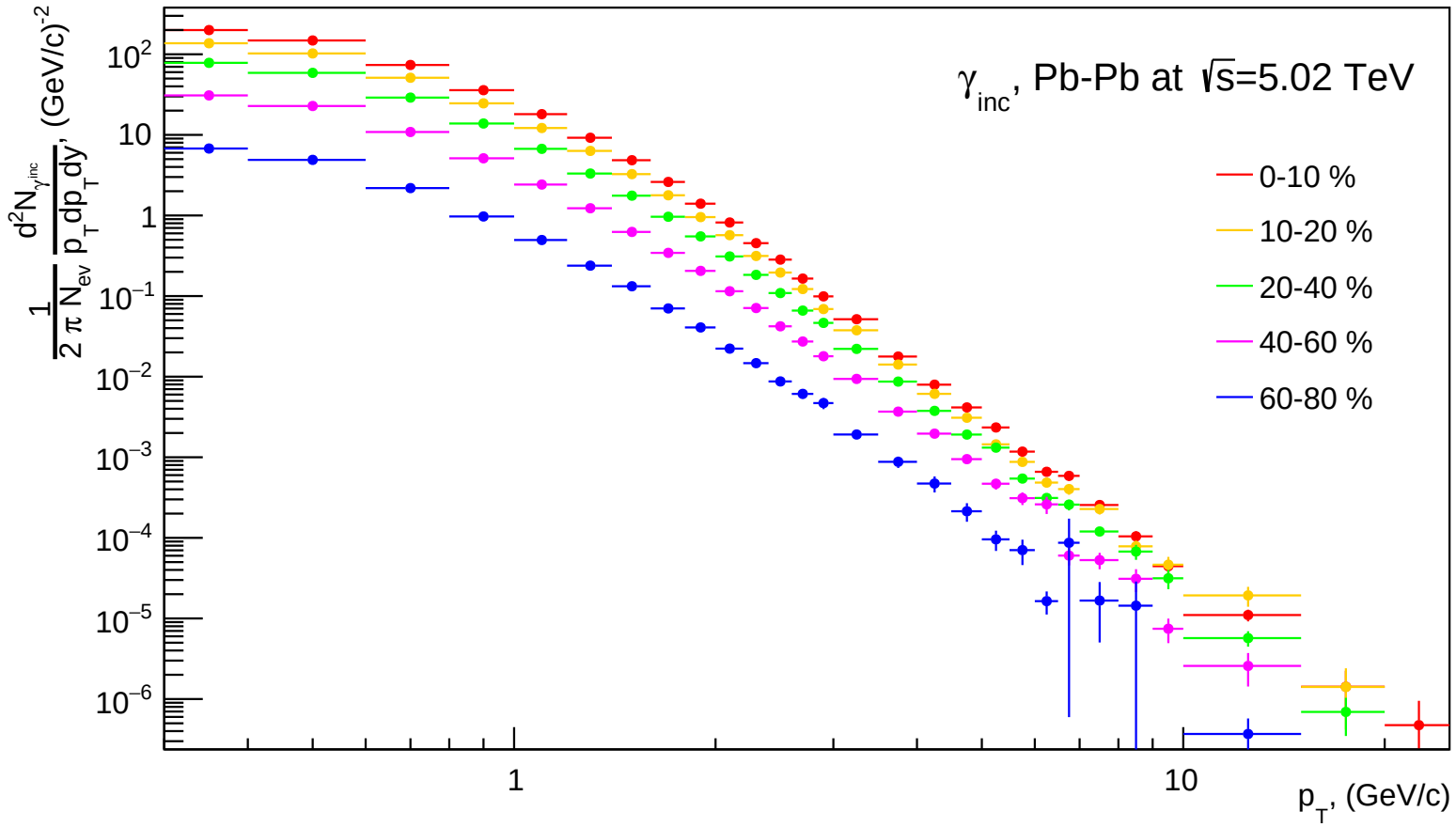

Background photon estimation using MC cocktail generation

Particle	Mass (MeV/c^2)	Decay channel	Branching ratio (%)
π^0	135	$\gamma\gamma$	98.8
		$\gamma e^+ e^-$	1.2
η	547	$\gamma\gamma$	39.2
		$\gamma\pi^+\pi^-$	4.8
		$\gamma e^+ e^-$	4.9×10^{-3}
ω	782	$\pi^0\gamma$	8.3
		$\eta\gamma$	4.6×10^{-4}
η'	958	$\rho^0\gamma$	29.1
		$\omega\gamma$	2.8

- **Hagedorn function** [2]: $\frac{d^2N}{dydp_T} = p_T \cdot A\left(\exp(ap_T + bp_T^2) + \frac{p_T}{p_0}\right)^{-n}$
  This functional form approaches an exponential at low p_T and a power law at larger transverse momenta and describes the measured spectra over full measured range
- **Transverse mass scaling :** $m_T = \sqrt{p_T^2 + m_0^2}$; $\frac{d^2N}{p_T dp_T dy} = \frac{d^2N}{m_T dm_T dy}$
  Transverse momenta spectra,
  $f_X(p_T, X) = C \times \frac{p_{T,X}}{\sqrt{m_{0,x}^2 + p_{T,x}^2 - m_{0,R}^2}} \times f_R(\sqrt{m_{0,x}^2 + p_{T,x}^2 - m_{0,R}^2})$

[2] Centrality determination in heavy ion collisions, ALICE Collaboration, 2018

Hadronic decay photon spectra using MC cocktail simulation

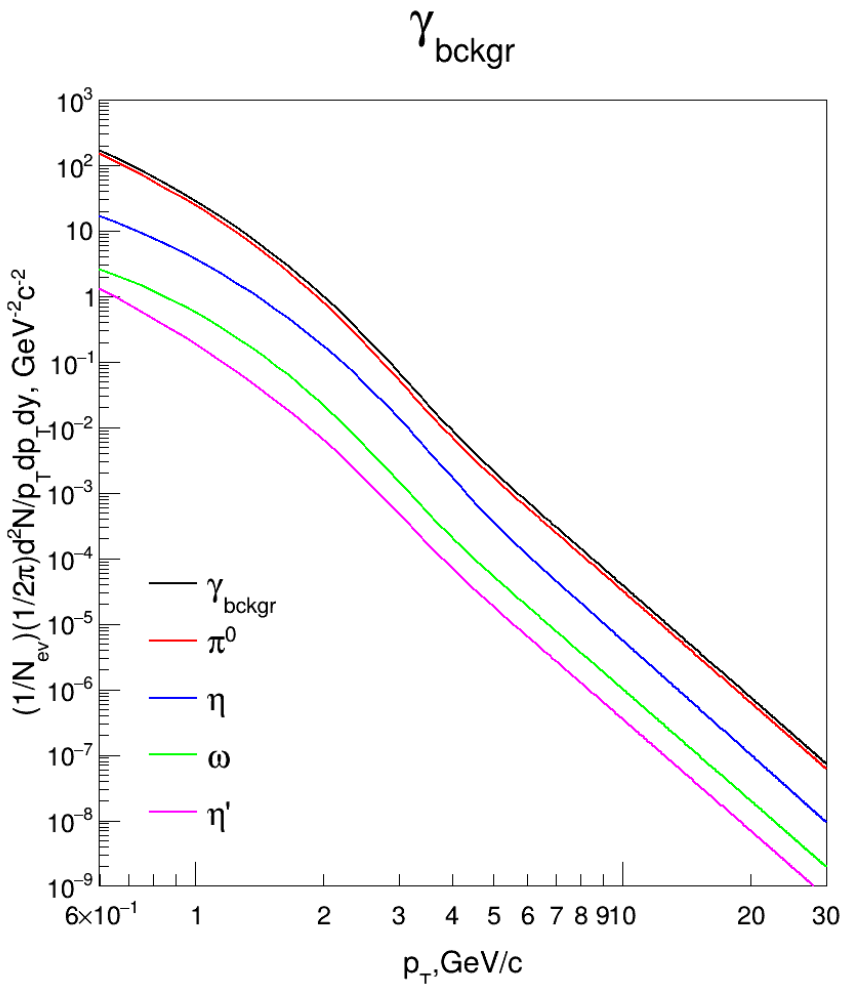

- π^0 and η mesons are generated using parametrization. ω and η' are generated using transverse mass scaling of π^0 spectra

Decay photon cocktail in Pb–Pb collisions at $\sqrt{s_{NN}} = 5.02$ TeV centrality 0-10 %

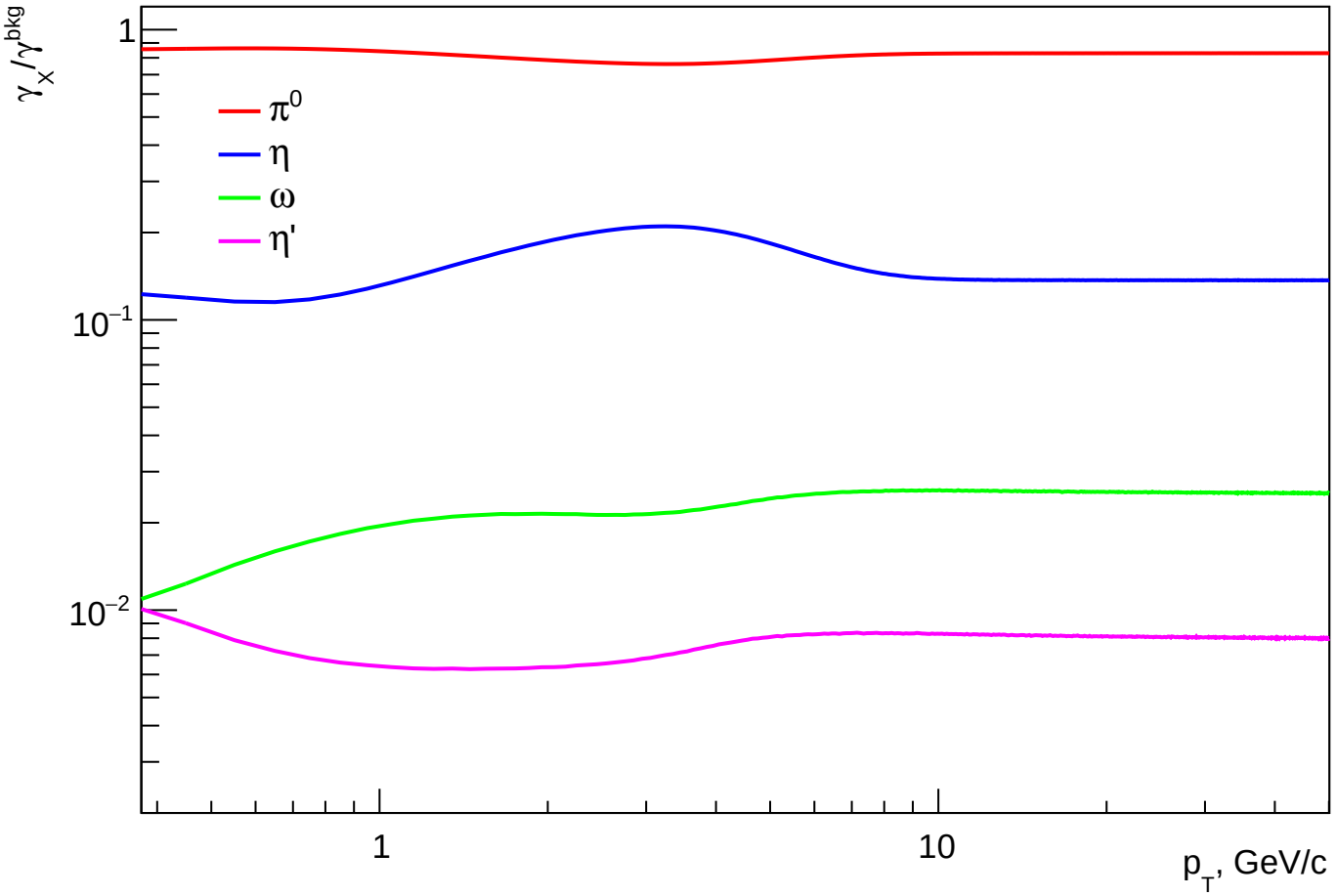

Figure: π^0 ($\sim$ 90%) is the most dominant background

Inclusive and decay photon spectra for centrality 0-10 %

compared with pertubative-QCD results (for different factorization scales)

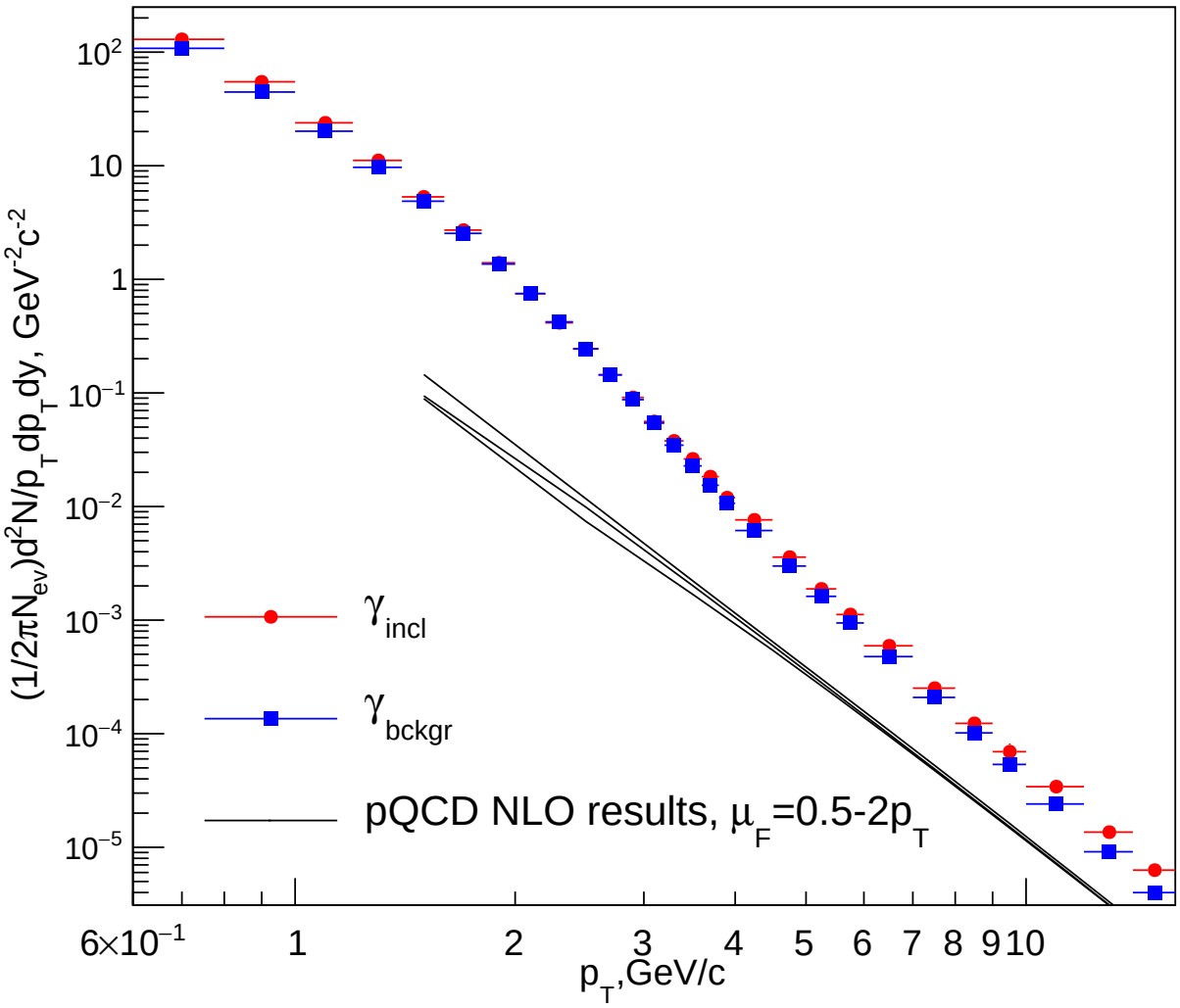

Direct photons(γ_{direct}) spectra using the Double ratio(R_D)

$$R_\gamma = \frac{\gamma^{\text{inc}}}{\gamma^{\text{decay}}} \approx \left(\frac{\gamma^{\text{inc}}}{\pi^0_{\text{meas}}}\right)_{\text{data}} \Big/ \left(\frac{\gamma^{\text{decay}}}{\pi^0_{\text{param}}}\right)_{\text{MC}} = R_D \tag{5}$$

$$\gamma_{\text{direct}} = \gamma_{\text{incl}} - \gamma_{\text{decay}} = \left(1 - \frac{1}{R_D}\right) \gamma_{\text{incl}} \tag{6}$$

Finally, the direct photons invariant yield can be calculated as follows,

$$\frac{1}{2\pi N_{\text{ev}}} \frac{d^2 N_{\gamma\, dir}}{p_{\text{T}} dp_{\text{T}} dy} = \frac{1}{2\pi N_{\text{ev}}} \frac{d^2 N_{\gamma\, inc}}{p_{\text{T}} dp_{\text{T}} dy} \left(1 - \frac{1}{R_D}\right) \tag{7}$$

γ/π^0 ratios for the calculation of the double ratio(R_D)

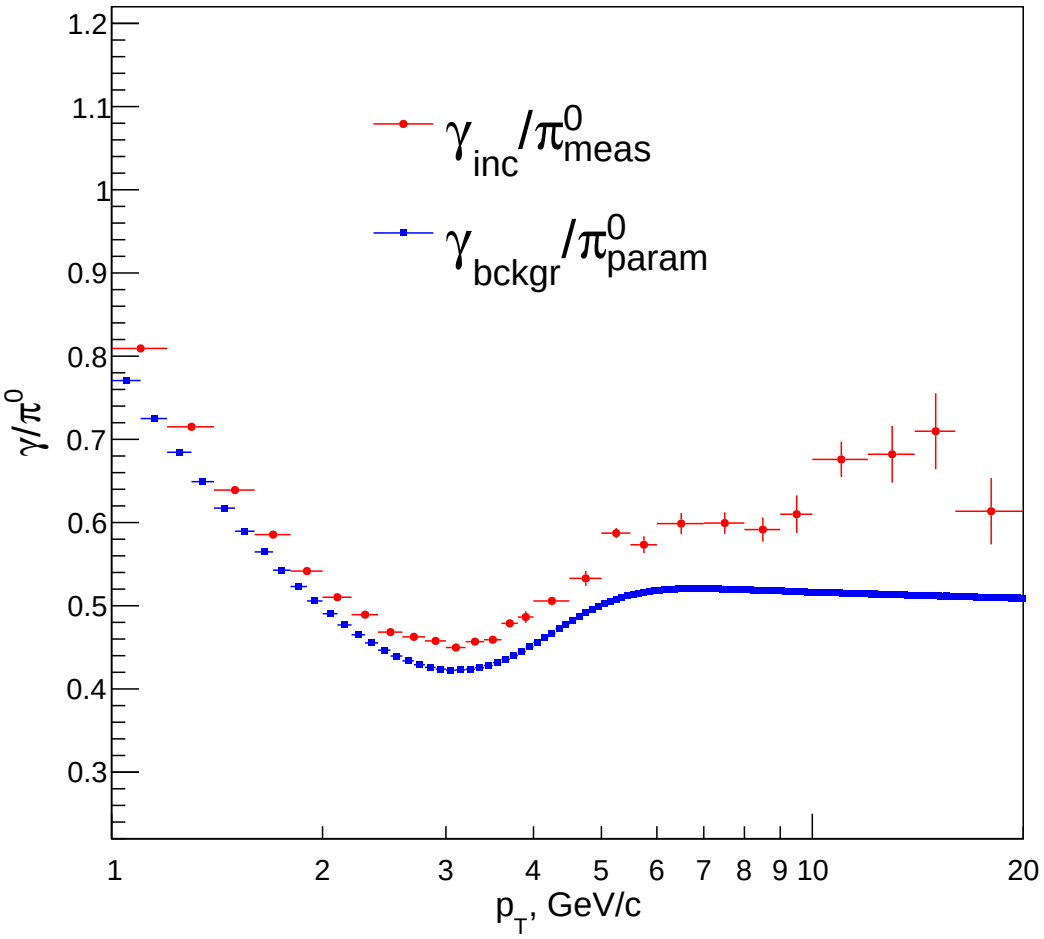

Figure: To be used for Double ratio

Double ratio for Pb-Pb at $\sqrt{s} = 5.02$ TeV, centrality 0-10%

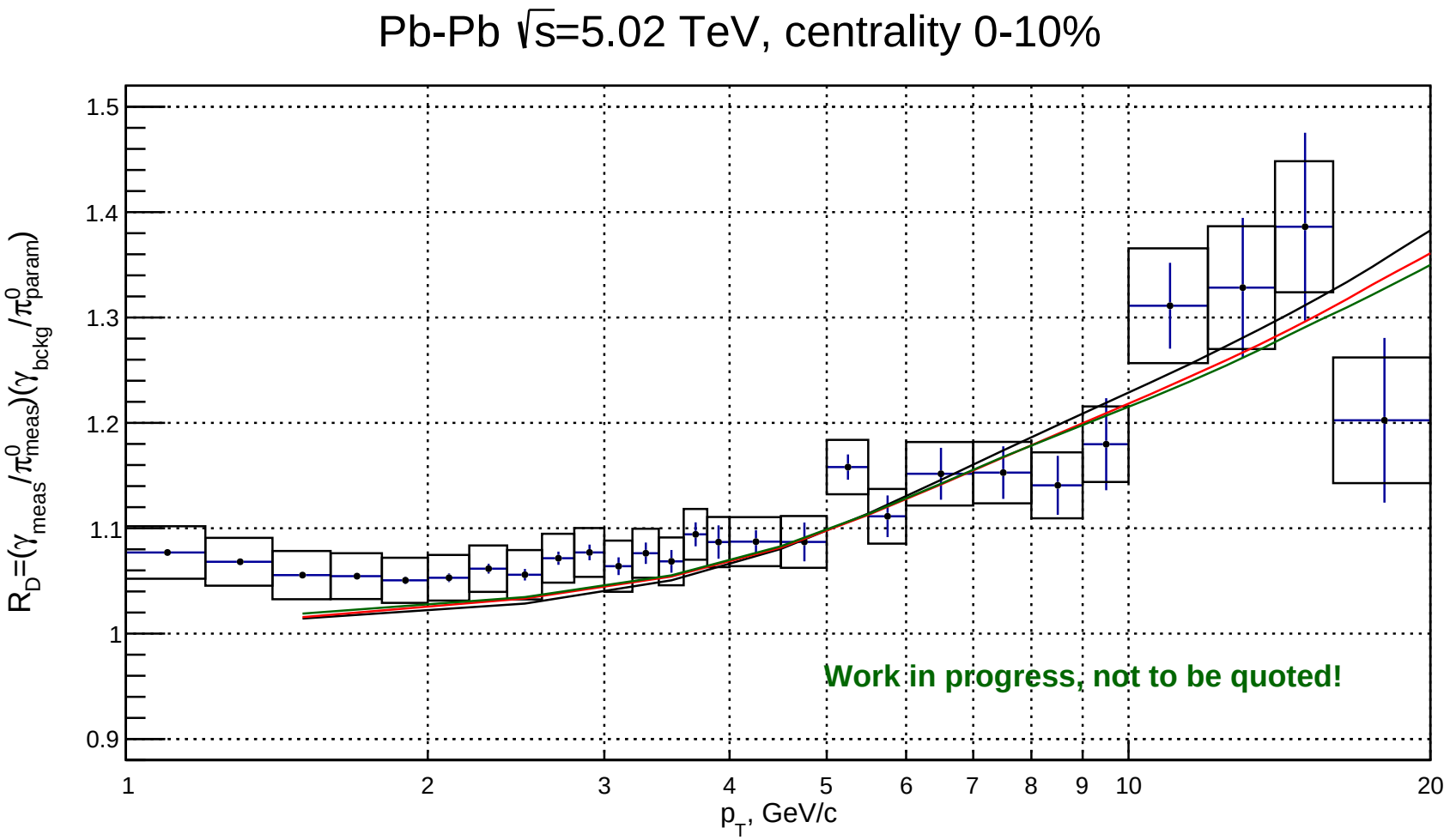

Figure: Black, red and green curves refer to the NLO pQCD predictions for factorization scales $\mu_F = 0.5, 1, 2p_T$, respectively.

Direct photon invariant yield and estimation of the effective temperature

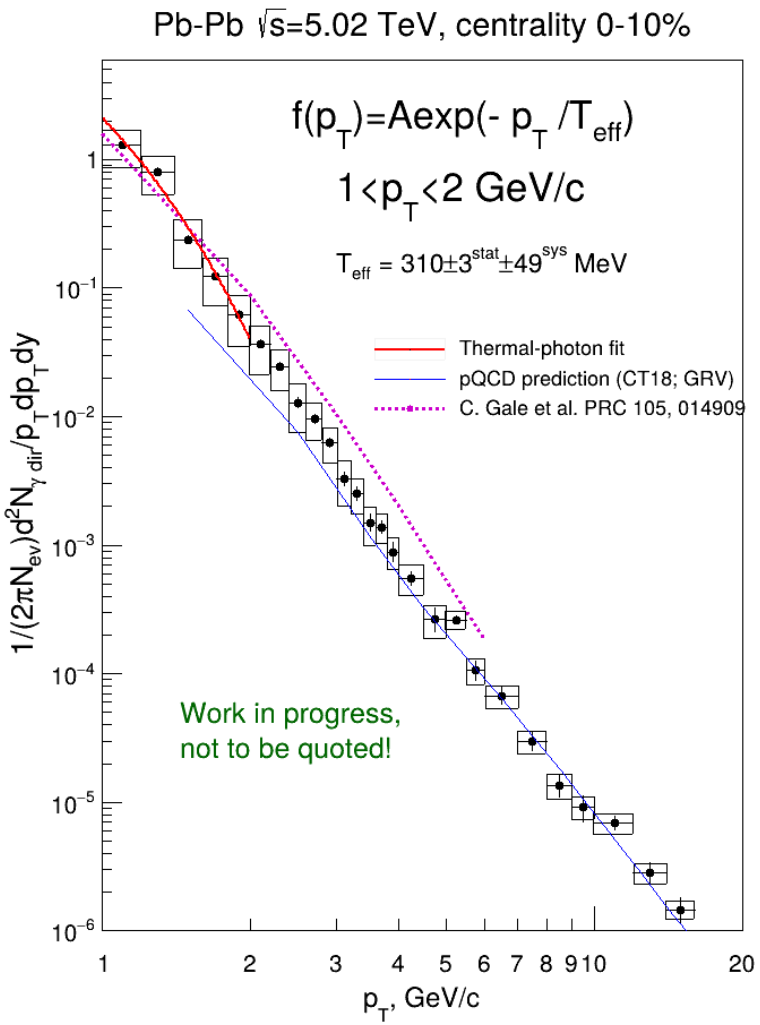

The invariant yield of direct photons demonstrates an **excess over the pQCD prediction**, which may indicate a presence of thermal photons.

We fit the invariant yield of the direct photons with an exponential function in the interval $1 < p_T < 2$ GeV/c

The effective temperature is the inverse slope of the exponent: $T_{\mathrm{eff}} = 310 \pm 3^{\mathrm{stat}} \pm 49^{\mathrm{sys}}$ MeV.

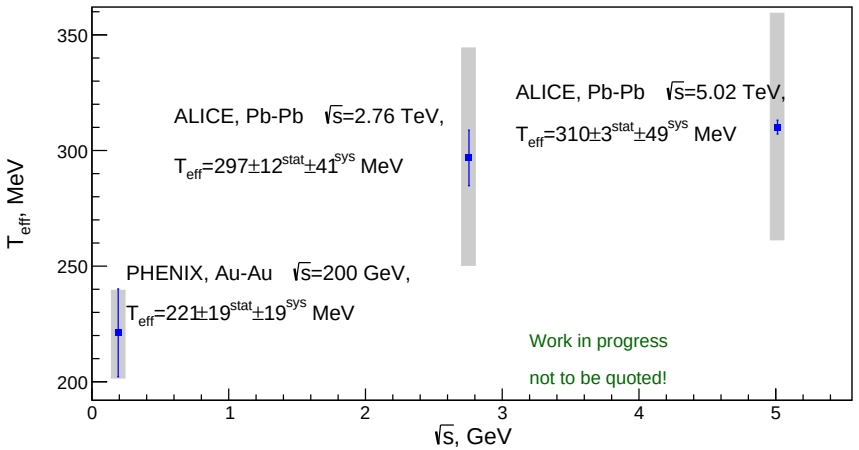

Fitting the difference between the measured direct photon invariant yield and the pQCD NLD predictions

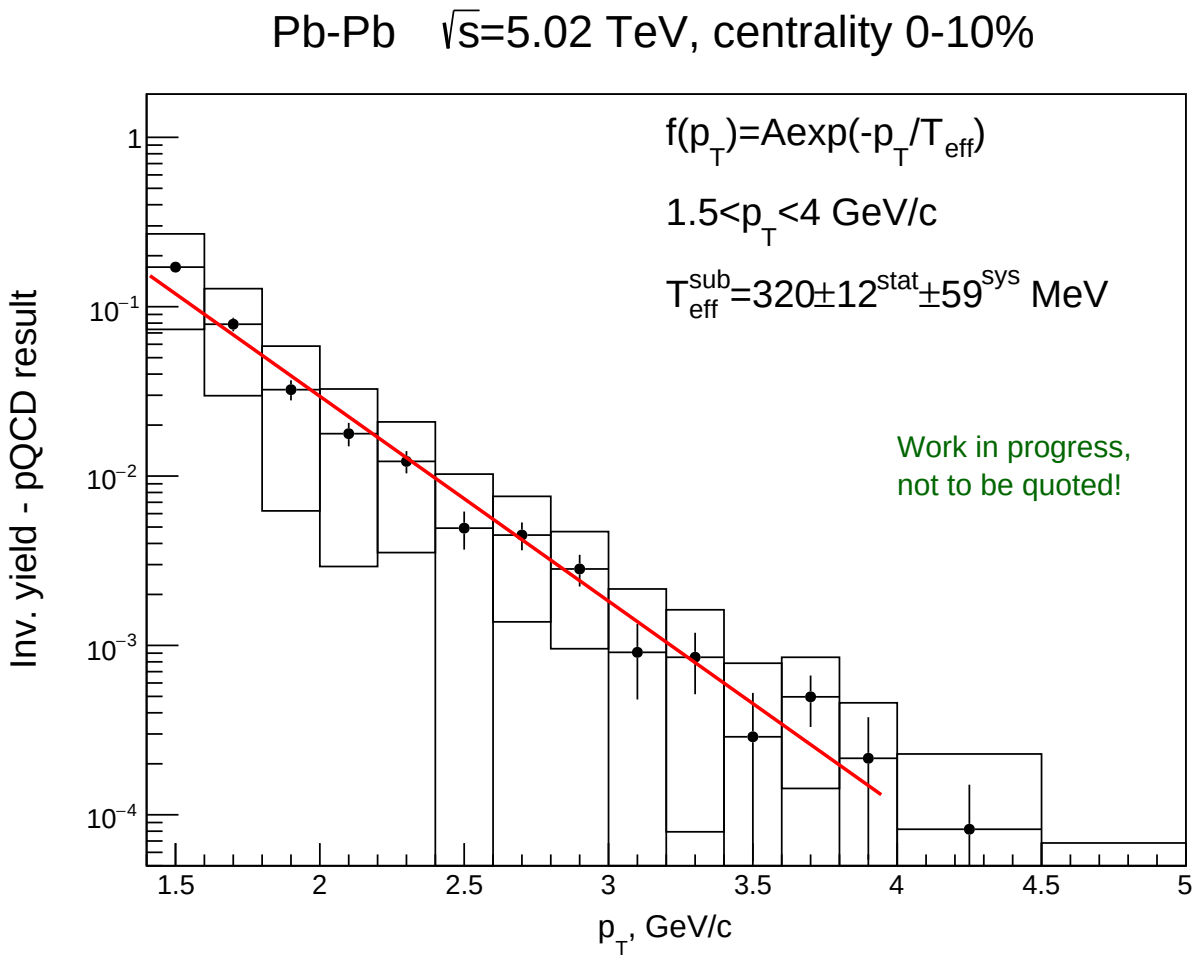

Figure: Thermal photons in low pT(1.5 GeV) to 4 GeV where pQCD results are available to estimate the average temperature of the medium

Summary: Preliminary analysis and Data-driven corrections

- **Inclusive and Decay photons**

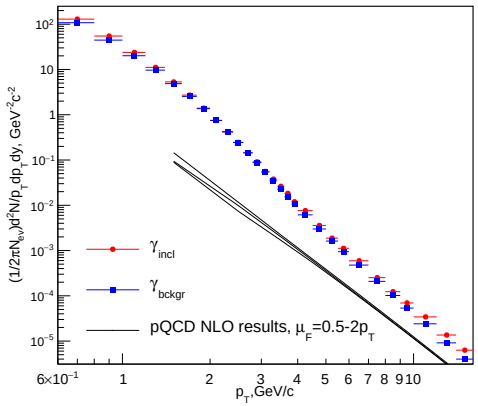

- **Direct photons**

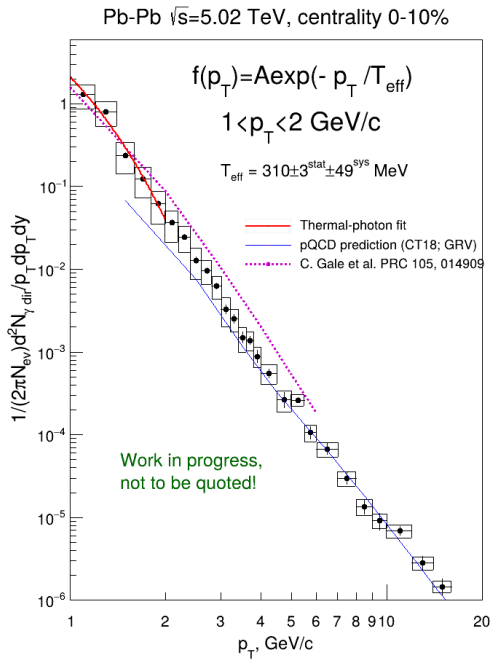

- **Efficiency from the Photon embedding technique**

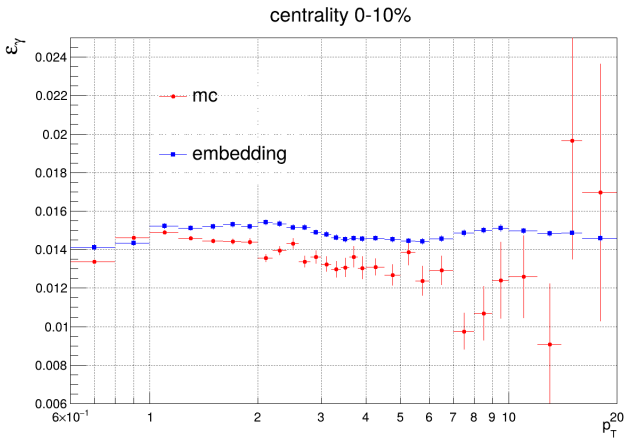

- **Ongoing ⇒ Purity from System of equations**

$$\begin{bmatrix} N^{\text{All}} \\ N^{\text{Disp}} \\ N^{\text{CPV}} \\ N^{\text{Both}} \end{bmatrix} = \begin{bmatrix} 1 & 1 & 2 & 1 \\ \varepsilon_\gamma^{\text{Disp}} & \varepsilon_\pi^{\text{Disp}} & 2\varepsilon_{\bar{p}}^{\text{Disp}} & \varepsilon_X^{\text{Disp}} \\ \varepsilon_\gamma^{\text{CPV}} & \varepsilon_\pi^{\text{CPV}} & \varepsilon_\pi^{\text{CPV}} + \varepsilon_\gamma^{\text{CPV}} & \varepsilon_X^{\text{CPV}} \\ \varepsilon_\gamma^{\text{Disp}}\varepsilon_\gamma^{\text{CPV}} & \varepsilon_\pi^{\text{Disp}}\varepsilon_\pi^{\text{CPV}} & \varepsilon_{\bar{p}}^{\text{Disp}}(\varepsilon_\pi^{\text{CPV}} + \varepsilon_\gamma^{\text{CPV}}) & \varepsilon_X^{\text{Disp}}\varepsilon_X^{\text{CPV}} \end{bmatrix} \begin{bmatrix} N_\gamma \\ N_{\pi^\pm} \\ N_{\bar{n}} \\ N_X \end{bmatrix}$$

BACKUP SLIDES

Reconstruction Workflow for PHOS Embedding

- **1. Signal simulation**
  Generate single photons (or π^0) with known p_T and η distributions. Transport them through the PHOS geometry using Geant to produce realistic **energy deposits (digits)**.
- **2. Real event preparation**
  Select real Pb–Pb events that provide the **background digits** — containing true detector noise, pileup, and occupancy.
- **3. Digit-level superposition**
  Combine the two sets of digits:
  $$D_{\text{embedded}}(i) = D_{\text{real}}(i) + D_{\text{signal}}(i)$$
  to form new raw data mimicking a photon embedded into a real event.
- **4. Reconstruction**
  Apply the standard PHOS reconstruction to the embedded digits: calibration, bad-channel masking, cluster building, and PID cuts $\rightarrow$ **embedded clusters**.
- **5. Efficiency extraction**
  Compare reconstructed embedded clusters to generated photons:
  $$\varepsilon_\gamma(p_T) = \frac{N_{\text{reco}}^{(\text{after embedding})} - N_{\text{reco}}^{(\text{before})}}{N_{\text{generated}}}$$
  giving a realistic efficiency $\times$ acceptance.

Embedding = simulate photon $\rightarrow$ add to real Pb–Pb digits $\rightarrow$ reconstruct $\rightarrow$ compare to generated.
Measures how well a real detector environment recovers true photons.

Data Driven Approach for Purity

- Data-driven approach (DDA): We define particle identification filters and the efficiency of the filters relative to different species of particles. It allows to build linear equation with the numbers of different particle clusters in each p_T-bin

$$\begin{bmatrix} N^{\text{All}} \\ N^{\text{Disp}} \\ N^{\text{CPV}} \\ N^{\text{Both}} \end{bmatrix} = \begin{bmatrix} 1 & 1 & 2 & 1 \\ \varepsilon_\gamma^{\text{Disp}} & \varepsilon_\pi^{\text{Disp}} & 2\varepsilon_{\bar{p}}^{\text{Disp}} & \varepsilon_X^{\text{Disp}} \\ \varepsilon_\gamma^{\text{CPV}} & \varepsilon_\pi^{\text{CPV}} & \varepsilon_\pi^{\text{CPV}} + \varepsilon_\gamma^{\text{CPV}} & \varepsilon_X^{\text{CPV}} \\ \varepsilon_\gamma^{\text{Disp}}\varepsilon_\gamma^{\text{CPV}} & \varepsilon_\pi^{\text{Disp}}\varepsilon_\pi^{\text{CPV}} & \varepsilon_{\bar{p}}^{\text{Disp}}(\varepsilon_\pi^{\text{CPV}} + \varepsilon_\gamma^{\text{CPV}}) & \varepsilon_X^{\text{Disp}}\varepsilon_X^{\text{CPV}} \end{bmatrix} \begin{bmatrix} N_\gamma \\ N_{\pi^\pm} \\ N_{\bar{n}} \\ N_X \end{bmatrix}$$

$$Purity(p_T) = \frac{N_\gamma(p_T)}{N^{all}(p_T)}$$

Anisotropic Flow

Asymmetry in the initial geometry → anisotropy in particle momenta distributions

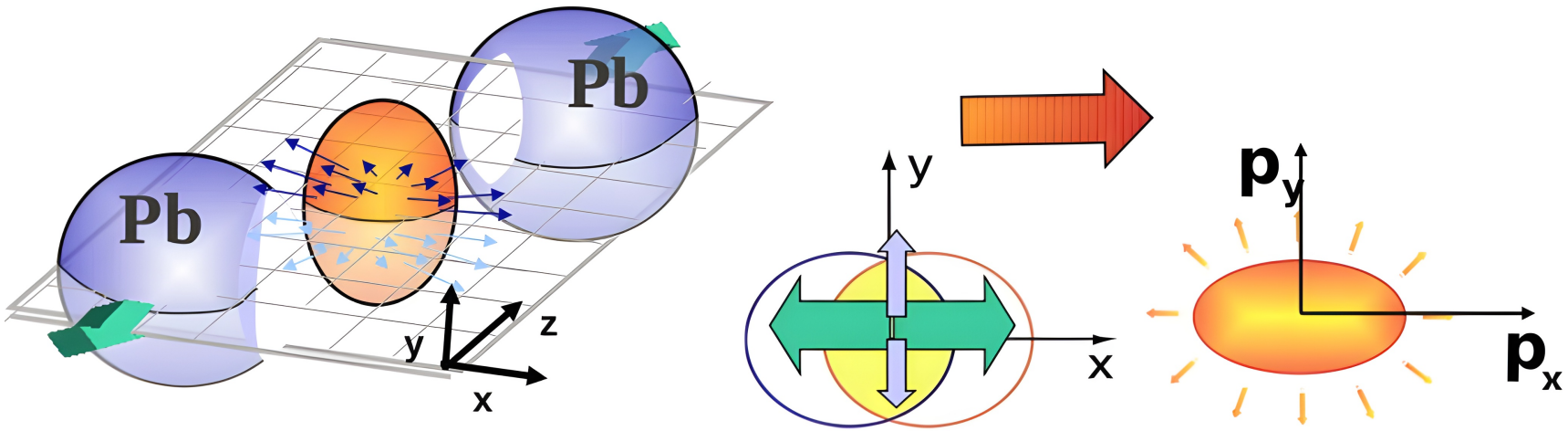

Azimuthal anisotropy can be described by Fourier expansion of particles' angular distribution around the beam direction:

$$E\frac{d^3N}{d^3\mathbf{p}} = \frac{1}{2\pi p_t}\frac{d^2N}{dp_t dy}\left(1 + 2\sum_{n=1}^{\infty} v_n \cos\left[n(\varphi - \Psi_{\mathrm{RP}})\right]\right) \tag{8}$$

where, v_1 (Directed flow), v_2 (Elliptic flow), v_3 (Triangular flow), ... are the Fourier coefficients.

Elliptic Flow of direct photons

$$v_{2,\mathrm{dir}} = \frac{R_\gamma v_{2,\mathrm{inc}} - v_{2,\mathrm{decay}}}{R_\gamma - 1} \tag{9}$$

where R_γ is the photon excess ratio, $v_{2,\mathrm{inc}}$ represents the inclusive flow, and $v_{2,\mathrm{decay}}$ is the decay photon flow.

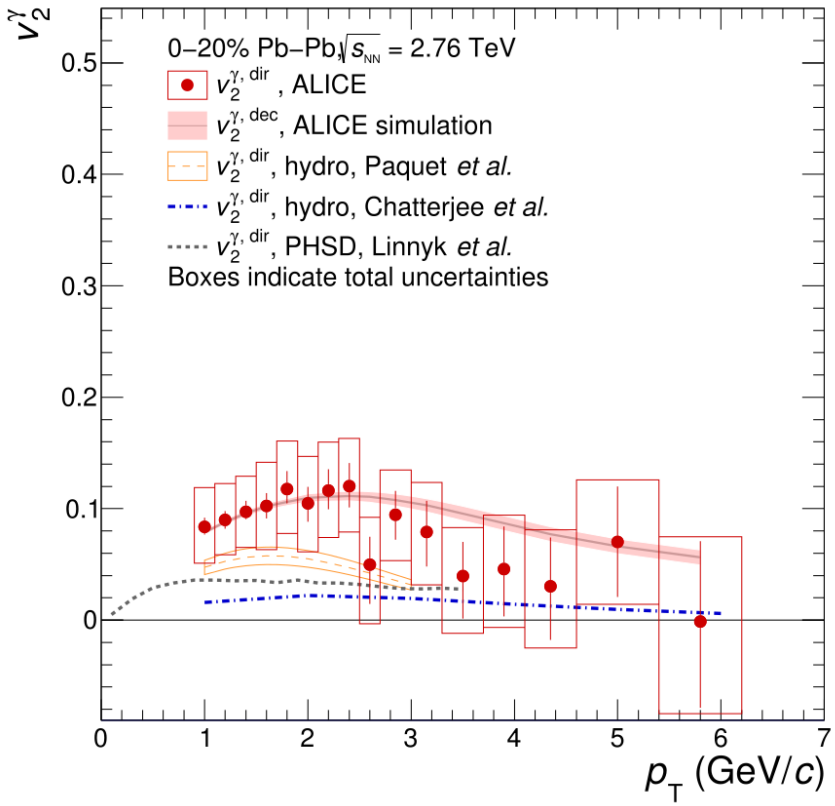

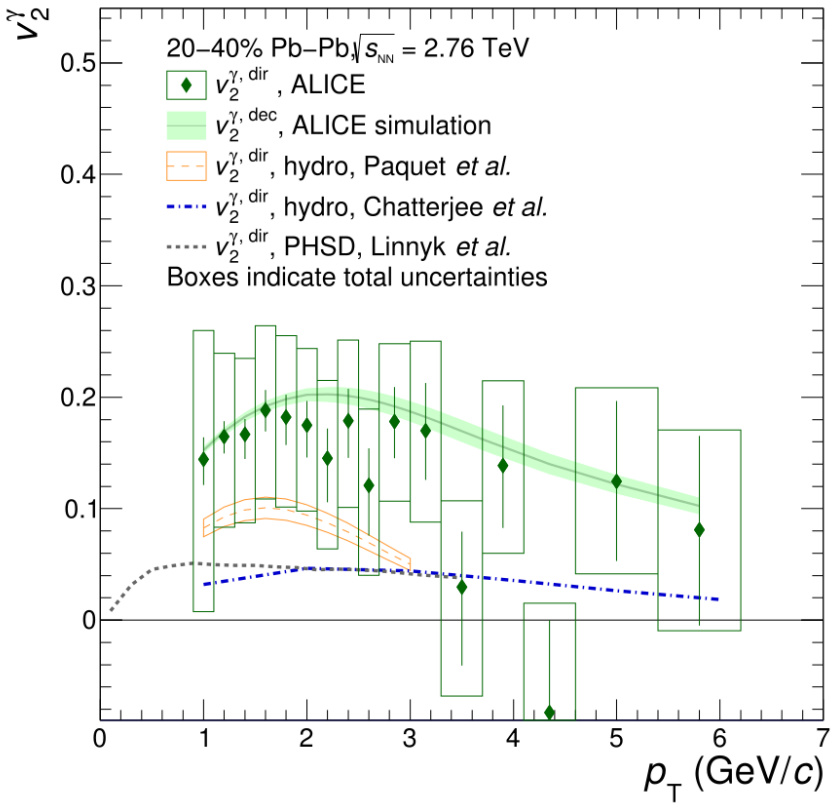

[3]

[3] Figure reference: *Physics Letters B 789 (2019) 308–322*

Direct Photon Puzzle

- Large direct photon yields and significant elliptic flow
- Contradiction between large photon yields (expected at early stages) and large anisotropy (expected at late stages).
- Theoretical models struggle to explain both yields and anisotropy simultaneously
- The ”direct photon puzzle” has inspired extensive theoretical work and new models

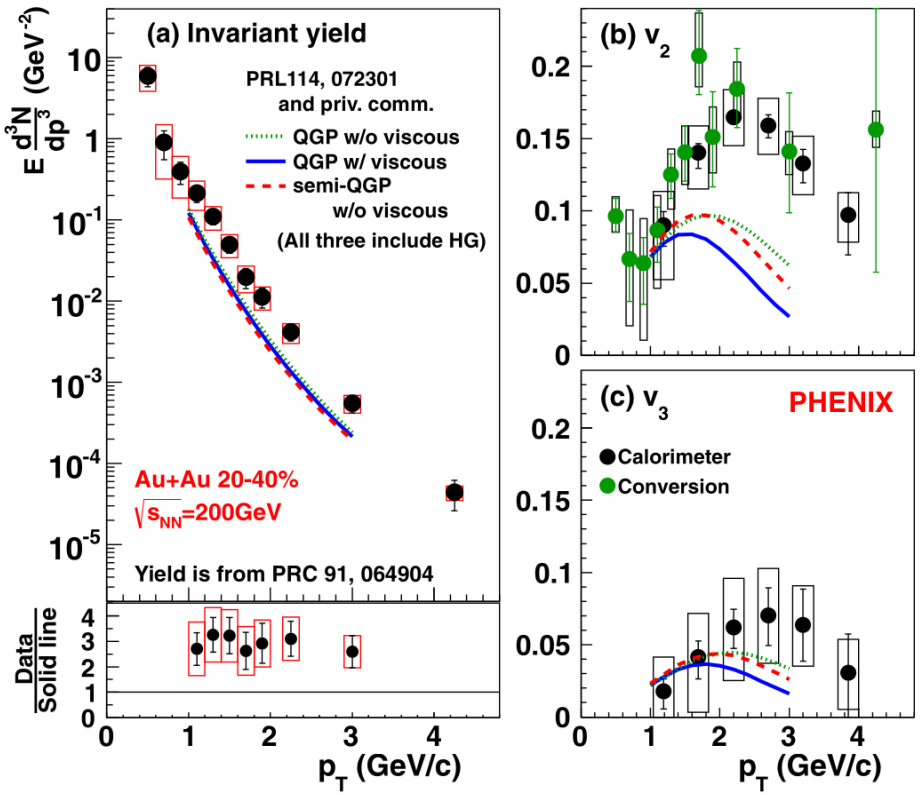

Double Ratio : To reduce systematic uncertainty

$$\text{Decay 1: } X \to A + B$$
$$\text{Decay 2: } X \to C + D$$

Problem: The detector has different efficiencies for detecting particles A, B, C, and D. This makes directly calculating the branching ratios inaccurate.

$T(X \to AB) =$ True number, $D(X \to AB) =$ Detected number, ε (A) etc.= Detection efficiencies

Single Ratio: The measured branching ratio of X decays would be:

$$\frac{D(X \to AB)}{D(X \to CD)} = \frac{\varepsilon(A) * \varepsilon(B) * T(X \to AB)}{\varepsilon(C) * \varepsilon(D) * T(X \to CD)}$$

Introducing a particle Y with similar decays and a known true branching ratio : R(Y) = $\frac{T(Y \to AB)}{T(Y \to CD)}$

Double Ratio:

$$\frac{D(X \to AB)/D(Y \to AB))}{D(X \to CD)/D(Y \to CD)}$$
$$= \frac{[\varepsilon(A)\varepsilon(B)T(X \to AB)]/[\varepsilon(A)\varepsilon(B)T(Y \to AB)]}{[\varepsilon(C)\varepsilon(D)T(X \to CD)]/[\varepsilon(C)\varepsilon(D)T(Y \to CD)]}$$

Difference in Single ratio vs double ratio (0-10% centrality)

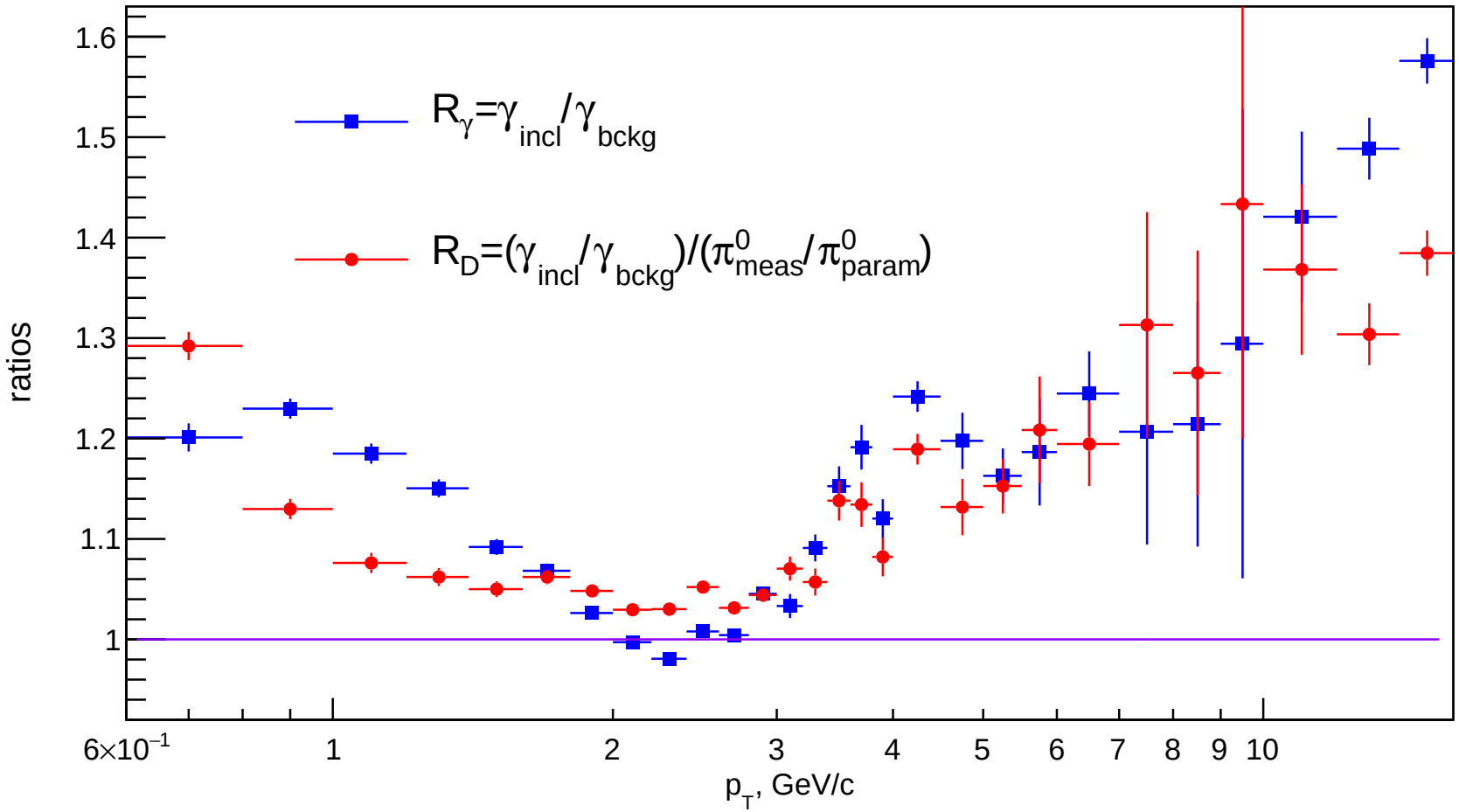

Difference in shape of π^0 ratios from data and MC for centrality 0-10 %

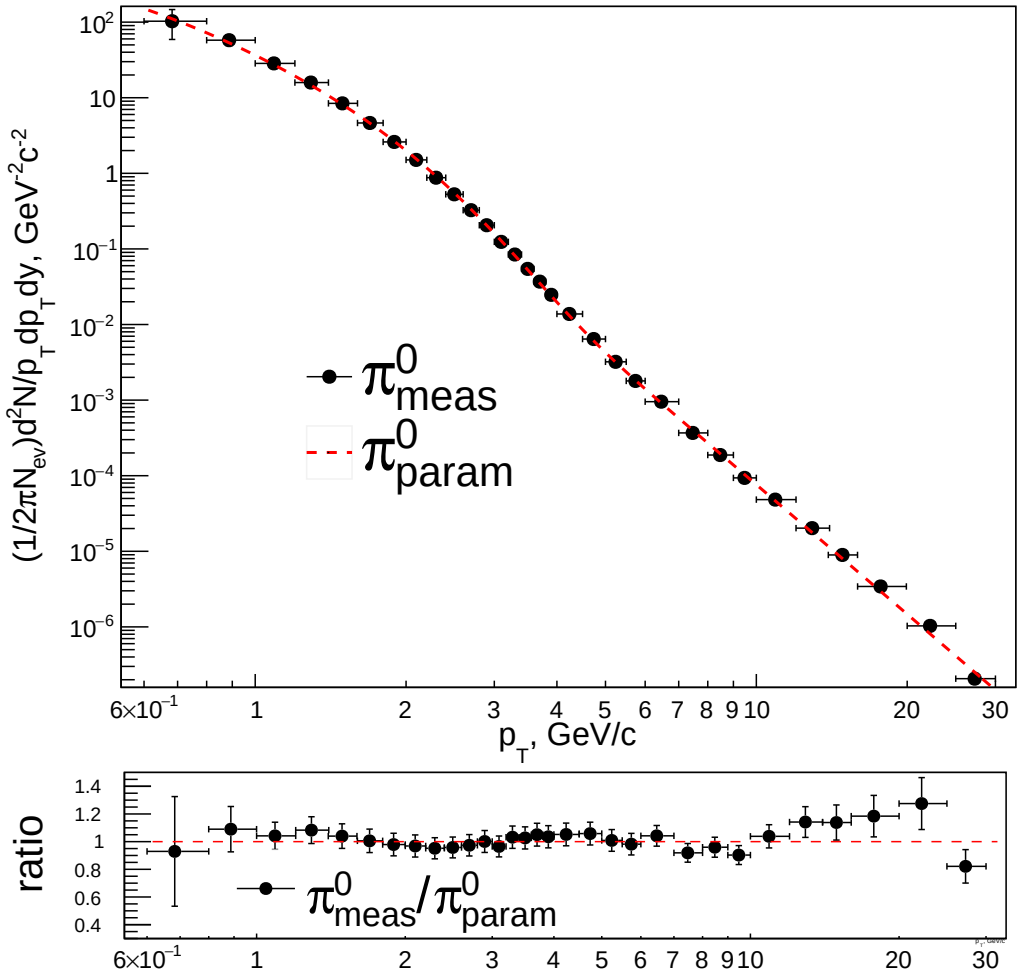

Double ratio for p-p at $\sqrt{s} = 13$ TeV

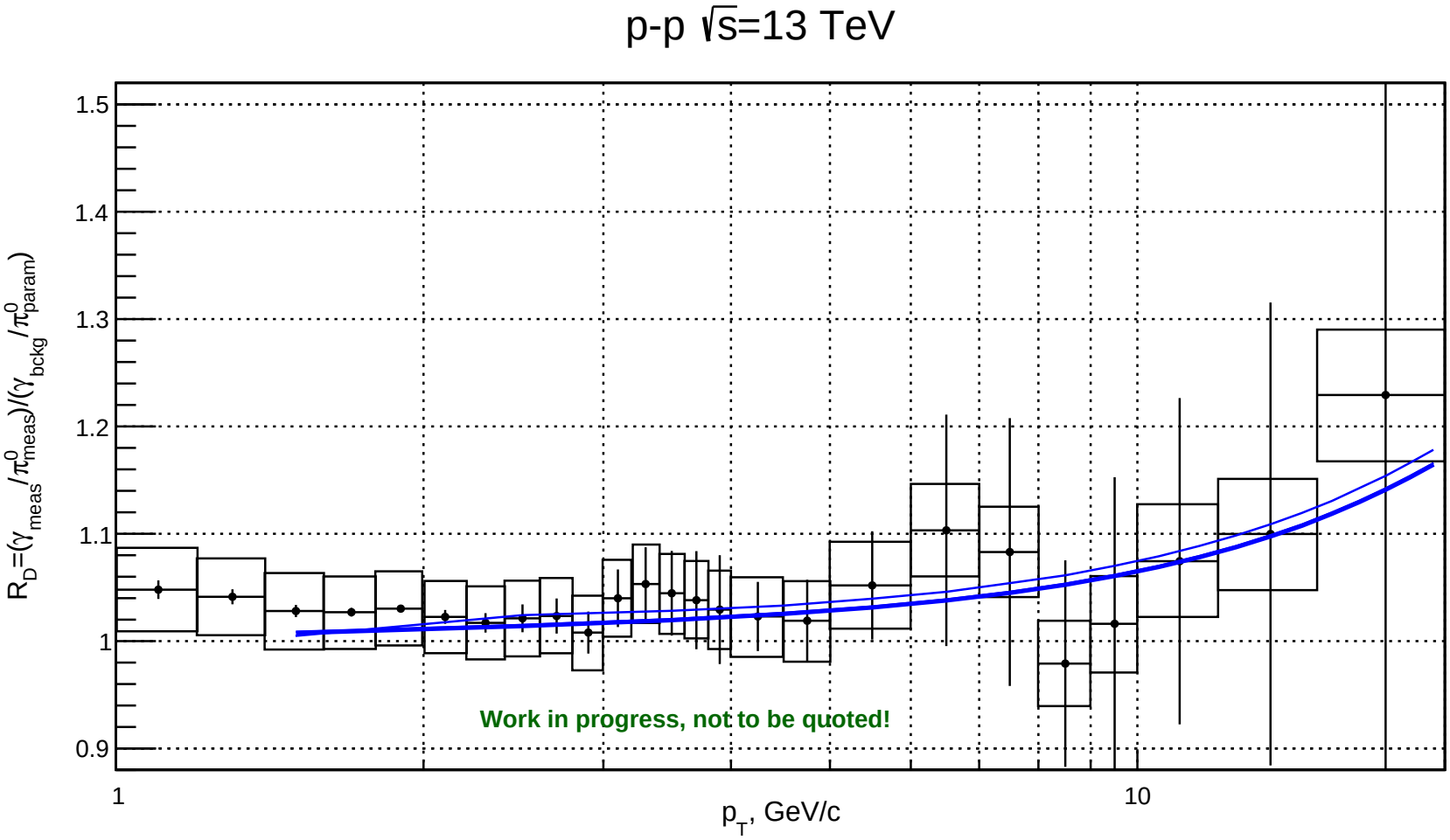

Figure: Double ratio for p-p collisions at $\sqrt{s} = 13$ TeV, statistical and systematic errors. The curves refer to the NLO pQCD predictions of prompt photon production for factorization scales $\mu_F = 0.5, 1, 2p_T$.

Double ratio systematic uncertainties, centrality 0-10%

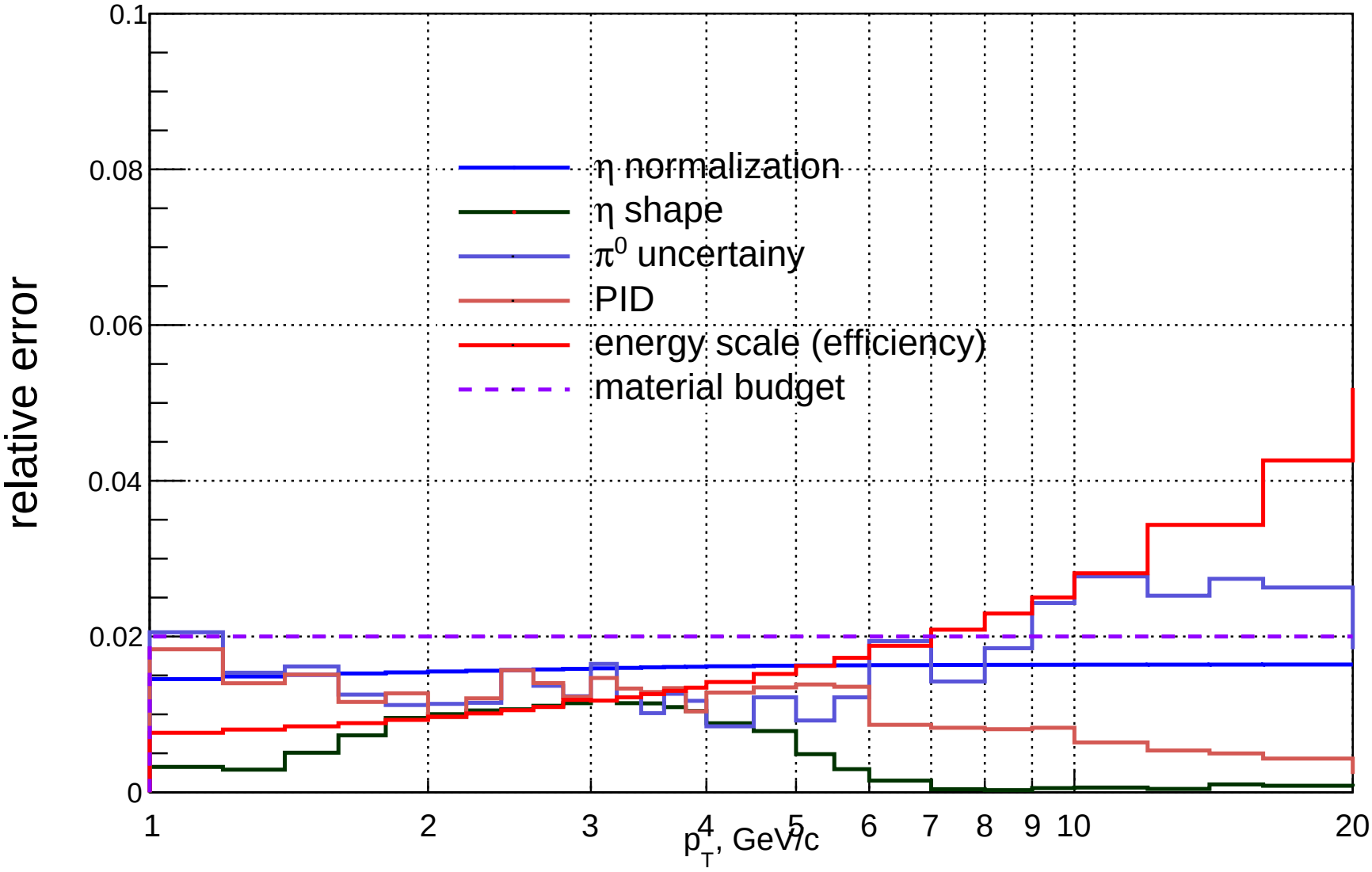

Advantages of nucleus-nucleus(e.g. Au, Cu, Pb) collisions over p-p collisions in the study of QCD phase diagram and QGP

- Energy density:
  - p-p collisions: Typically a few GeV/fm^3
  - A-A collisions: 10-20 GeV/fm^3 or higher
- Temperature:
  - A-A collisions: Several hundred MeV to over a trillion degrees Kelvin
- Size and lifetime of the QGP:
  - p-p collisions: Highly transient and smaller in size
  - A-A collisions: Spatial extent of several femtometers, lasting tens to hundreds of femtoseconds
- Particle multiplicity:
  - A-A collisions: Significantly larger number of particles compared to p-p collisions
- Jet quenching:
  - A-A collisions: Much more pronounced, resulting in stronger energy loss and modification of jet-related observables

Coordinate system in ALICE

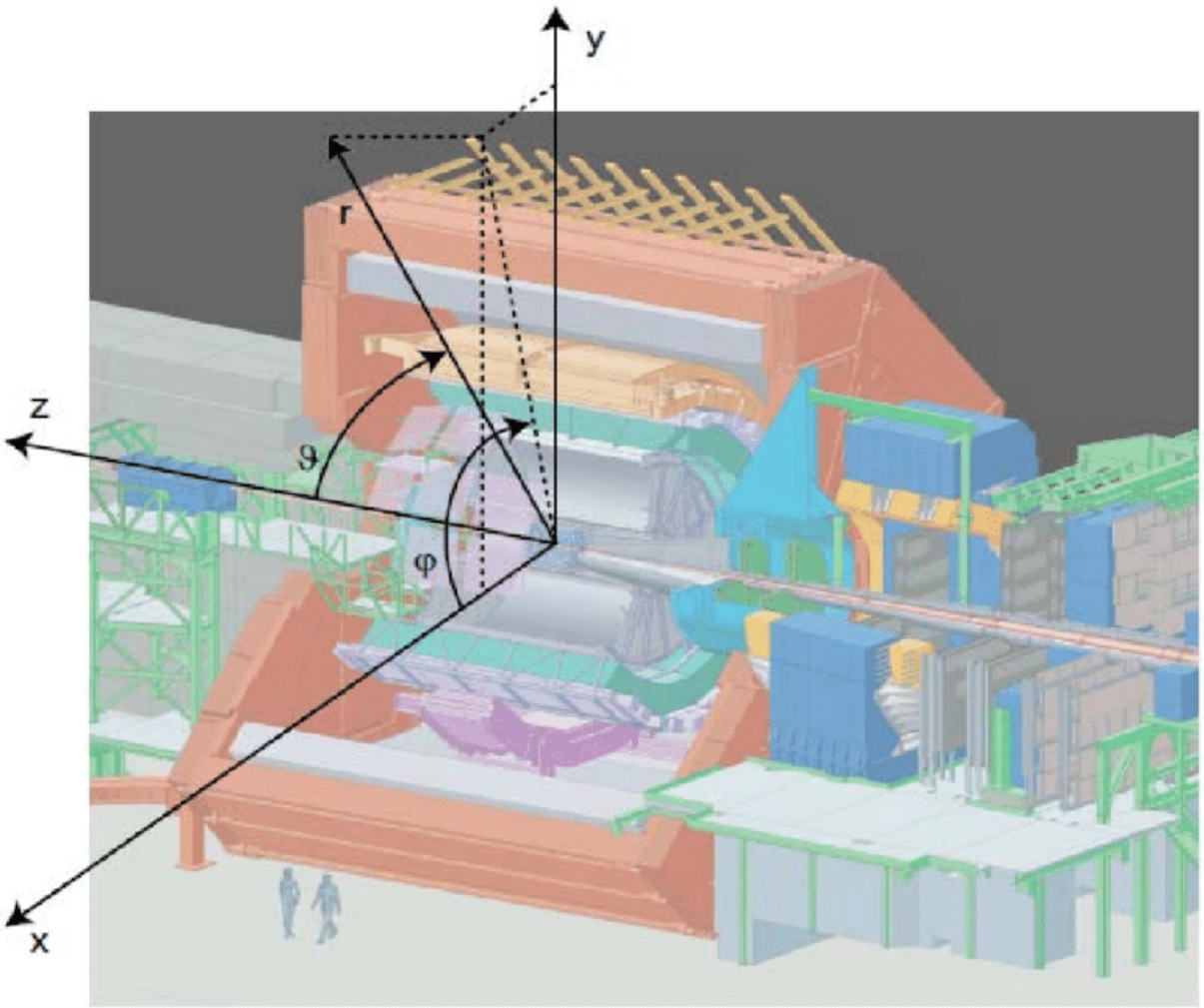

Figure: Like other major experiments at LHC, (θ, ϕ, z) co-ordinate system is used at ALICE . Pseudo-rapidity $\eta = -ln(tan\frac{\theta}{2})$

[3] https://doi.org/10.1016/j.cpc.2021.108206